The Pseudokinase Ulk4 promotes Shh signaling by regulating Stk36 ciliary localization and Gli2 phosphorylation

Mengmeng Zhou[1], Yuhong Han[1], and Jin Jiang[1,2,*]

[1]Department of Molecular Biology, [2]Department of Pharmacology, University of Texas Southwestern Medical Center, Dallas, TX 75390, USA

*Corresponding authors: jin.jiang@utsouthwestern.edu

Running title: Ulk4 promotes Gli phosphorylation and Hh signaling

Summary

The Hedgehog (Hh) family of secreted proteins governs embryonic development and adult tissue homeostasis through the Gli family of transcription factors. Gli is thought to be activated at the tip of primary cilium, but the underlying mechanism remains poorly understood. Here, we show that Unc-51-like kinase 4 (Ulk4), a pseudokinase and a member of the Ulk kinase family, acts in conjunction with another Ulk family member Stk36 to promote Gli2 phosphorylation and Hh pathway activation. Ulk4 interacts with Stk36 through its N-terminal region containing the pseudokinase domain and Gli2 via its regulatory domain to bridge the kinase and substrate. Although dispensable for Hh-induced Stk36 kinase activation, Ulk4 is essential for Stk36 ciliary tip localization, Gli2 phosphorylation and activation. In response to Hh, both Ulk4 and Stk36 colocalize with Gli2 at ciliary tip, and Ulk4 and Stk36 depend on each other for their ciliary tip accumulation. We further show that ciliary localization of Ulk4 depends on Stk36 kinase activity and phosphorylation of Ulk4 on Thr1023, and that ciliary tip accumulation of Ulk4 is essential for its function in the Hh pathway. Taken together, our results suggest that Ulk4 regulates Hh signaling by promoting Stk36-mediated Gli2 phosphorylation and activation at ciliary tip.

Introduction

Pseudokinases, which comprise ~10% of the mammalian kinome, play essential biological functions yet the mechanism of action for many pseudokinases has remained unknown (Jacobsen and Murphy, 2017). One such pseudokinase is Unc-51-like kinase 4 (Ulk4), which is a member of Ulk kinase family found in most eukaryotes (Luo et al., 2022). The Ulk family kinases, which include Ulk1 (Atg1 in yeast) and Ulk2 involved in autophagy initiation, contain a conserved kinase domain in their N-terminal regions and a variable regulatory domain in their C-terminal regions (Luo *et al.*, 2022). However, unlike other Ulk family members, Ulk4 contains a pseudokinase domain at its N-terminus and is predicted to be catalytically inactive (Preuss et al., 2020). Ulk4 plays a key role in neurogenesis in mice by regulating neural stem cell pool and neurite branching morphogenesis (Lang et al., 2014; Liu et al., 2016a). In addition, Ulk4 regulates the integrity of white matter by promoting myelination (Liu et al., 2018b). Recent studies have implicated Ulk4 as a risk factor for neuropsychiatric disorders including schizophrenia (Lang *et al.*, 2014; Lang et al., 2016; Liu et al., 2018a; Luo *et al.*, 2022). However, the signaling pathways in which Ulk4 is involved and the substrates it regulates have remained unknown. A recent proteome study has revealed that Ulk4 interacts with Stk36 in additional to many other proteins (Preuss *et al.*, 2020). Stk36 is also a member of the Ulk family and mammalian homolog of *Drosophila* Fused (Fu), a Ser/Thr kinase implicated in Hedgehog (Hh) signaling (Han et al., 2019; Murone et al., 2000; Wilson et al., 2009). A recent study identified Ulk4 as a genetic modifier of the holoprosencephaly phenotype caused by impaired Shh pathway activity (Mecklenburg

69 et al., 2021). These observations have raised an interesting possibility that Ulk4 may
70 participate in Hh signal transduction.
71 The Hh family of secreted proteins governs embryonic development and adult tissue
72 homeostasis and deregulation of Hh signaling activity has been implicated in a myriad
73 of human disorders including birth defect and cancer (Briscoe and Therond, 2013;
74 Jiang, 2021; Jiang and Hui, 2008; Villavicencio et al., 2000). Hh exerts its biological
75 influence via an evolutionarily conserved signaling cascade that culminates in the
76 activation of Gli family of Zn-finger transcription factors. The core Hh signal reception
77 system consists of two multi-span transmembrane proteins Patched (Ptc) and
78 Smoothened (Smo) that transduce vertebrate Hh signal at primary cilia (Goetz and
79 Anderson, 2010). In quiescent cells, Ptc localizes to primary cilia where Smo is barely
80 detectable (Corbit et al., 2005; Rohatgi et al., 2007); the full-length Gli (Gli^F) undergoes
81 ubiquitin/proteasome-mediated proteolytic processing to generate a truncated
82 transcriptional repressor form (Gli^R) (Chen and Jiang, 2013; Jiang, 2002; Tempe et al.,
83 2006; Wang et al., 2000; Wang and Li, 2006). Hh inhibits Ptc activity and promotes its
84 ciliary exit, allowing Smo and Gli proteins to accumulate in the cilia to transduce the Hh
85 signal (Chen et al., 2009; Chen et al., 2011; Corbit *et al.*, 2005; Haycraft et al., 2005;
86 Rohatgi *et al.*, 2007; Tukachinsky et al., 2010). Activated Smo blocks the proteolytic
87 processing of Gli into Gli^R and converts Gli^F to an active form (Gli^A) that enters the
88 nucleus to turn on the expression of Hh target genes (Arveseth et al., 2021; Han *et al.*,
89 2019; Kim et al., 2009; Tukachinsky *et al.*, 2010; Wang *et al.*, 2000).
90 Although it is generally thought that Smo converts Gli^F into Gli^A at ciliary tip (Goetz
91 and Anderson, 2010), the underlying mechanism has remained an enigma. Our recent

92 studies have demonstrated that two Ulk family kinases Ulk3 and Stk36 play a role in
93 converting Gli^F into Gli^A by directly phosphorylating Gli2 at multiple sites in mammalian
94 cells (Han *et al.*, 2019; Zhou et al., 2022; Zhou and Jiang, 2022). Here, we provide
95 evidence that Ulk4 acts in conjunction with Stk36 to promote Gli2 phosphorylation and
96 Hh pathway activation. We show that Ulk4 interacts with Stk36 through its N-terminal
97 region containing the pseudokinase domain and with Gli2 via its C-terminal regulatory
98 domain to bring Stk36 and Gli2 into proximity. We find that Ulk4 is not required for Stk36
99 kinase activation by Shh but is essential for Stk36 ciliary localization and Gli2
100 phosphorylation. We show that, in response to Shh stimulation, both Ulk4 and Stk36
101 colocalize with Gli2 at the tips of primary cilia, and that Ulk4 and Stk36 depend on each
102 other for their ciliary tip accumulation. We further show that ciliary tip localization of Ulk4
103 depends on Stk36-mediated phosphorylation of Ulk4 on Thr1023, and that ciliary tip
104 localization of Ulk4 is essential for its function in Hh signal transduction.
105
106
107 **Results**
108
109
110 **Ulk4 acts in conjunction with Stk36 to promote Gli2 phosphorylation and Hh**
111 **pathway activation**
112
113 To determine whether Ulk4 is required for Hh pathway activation, we depleted Ulk4 by
114 RNA interference (RNAi) in NIH3T3 cells, a well-established system for studying Hh
115 signaling. We found that Ulk4 depletion significantly decreased Shh-induced expression
116 of *Gli1* and *Ptch1* determined by RT-qPCR, which was rescued by the expression of
117 human Ulk4 (hUlk4; Figure 1A-B; Figure 1-figure supplement 1). The requirement of

118 Ulk4 in Shh-induced expression of *Gli1* and *Ptch1* was confirmed in MEF cells (Figure
119 1-figure supplement 2).
120 Our previous study revealed that Stk36 and Ulk3, which are Ulk family kinases,
121 act in parallel to promote Gli2 phosphorylation and Hh pathway activation (Han *et al.*,
122 2019). To determine the relationship between Ulk4 and Ulk3/Stk36, we carried out
123 double RNAi experiments. We found that double knockdown (KD) of Ulk4 and Ulk3
124 further decreased Shh target gene expression compared with single KD of either Ulk4
125 or Ulk3 whereas double KD of Ulk4 and Stk36 did not have an additive effect (Figure
126 1C-D; Figure 1-figure supplement 2). These results indicated that Ulk4 acts in the same
127 pathway with Stk36 but in parallel with Ulk3 to promote Hh signaling.
128 Our previous study demonstrated that Ulk3 and Stk36 phosphorylate Gli2 at
129 multiple sites including S230/232 to promote Gli2 activation (Han *et al.*, 2019; Zhou *et*
130 *al.*, 2022). We found that Ulk4 KD reduced Gli2 phosphorylation on S230/232 stimulated
131 by Shh in NIH3T3 cells, which was determined by western blot analysis using a
132 phospho-specific antibody that recognizes pS230/232 (Han and Jiang, 2021; Han *et al.*,
133 2019), and that expression of hUlk4 restored Gli2 phosphorylation on S230/232 in Ulk4
134 depleted cells (Figure 1E). Consistent with Ulk4 acting in a liner pathway with Stk36 but
135 in parallel with Ulk3, double KD of Ulk4 and STK36 decreased S230/232
136 phosphorylation similarly to single KD of either Ulk4 or Stk36 whereas double KD of
137 Ulk3 and Ulk4 further decreased Shh-induced S230/232 phosphorylation compared with
138 single KD of Ulk3 or Ulk4 (Figure 1F-G). Taken together, these results demonstrated
139 that Ulk4 and Stk36 act in a linear pathway but in parallel with Ulk3 to participate in Hh
140 transduction by facilitating Gli2 phosphorylation and activation (Figure 1H).

141
142
143 **Ulk4 forms a complex with Stk36 and Gli2**
144
145
146 A previous study using proximity-dependent biotin identification (BioID) identified Stk36
147 as a proximity interactor (Preuss *et al.*, 2020). To verify that Stk36 formed a complex
148 with Ulk4, we carried out coimmunoprecipitation (Co-IP) experiments and found that a
149 C-terminal HA-tagged Ulk4 (hUlk4-HA) interacted with a N-terminal CFP-tagged Stk36
150 (CFP-Stk36) in HEK293T cells (Figure 2A). To explore whether Ulk4 interacted with Gli2
151 and Sufu, a Gli binding partner and Hh pathway inhibitor (Cooper et al., 2005; Dunaeva
152 et al., 2003; Han et al., 2015), we co-expressed hUlk4-HA, with a Myc-tagged Gli2
153 (Myc-Gli2) and a Flag-tagged Sufu (Fg-Sufu) in HEK293T cells. Co-IP experiments
154 showed that both Myc-Gli2 and Fg-Sufu were pulled down by Ulk4-HA (Figure 2B),
155 suggesting that Ulk4 could form a complex with Stk36 and Gli2-Sufu.
156 Ulk4 contains an N-terminal pseudokinase domain and the C-terminal regulatory
157 domain with armadillo (Arm) repeats (Figure 2C) (Preuss *et al.*, 2020). We generated
158 two truncated forms of Ulk4: hUlk4N (aa 1-450) that contains the pseudokinase domain
159 and hUlk4C (451-1275) that contains the C-terminal regulatory domain. Co-IP
160 experiments showed that hUlk4N-HA interacted with CFP-Stk36 but not with Myc-
161 Gli2/Fg-Sufu whereas hUlk4C-HA formed a complex with Myc-Gli2/Fg-Sufu but not with
162 CFP-Stk36 (Figure 2D-E), suggesting that Ulk4 interacted with Stk36 and Gli2-Sufu
163 through its N-terminal pseudokinase domain and C-terminal regulatory domain,
164 respectively. Consistent with our observation, previous BioID experiments using BirA*-
165 Ulk4 pseudokinase domain also identified Stk36 as a proximity binding partner of the
166 Ulk4 pseudokinase domain (Preuss *et al.*, 2020).

167 **Ulk4 is dispensable for Shh-induced Stk36 kinase activation**
168
169
170 Pseudokinases could regulate the enzymatic activity of interacting kinases, as has been
171 shown for LKB1 kinase activation by its binding to the pseudokinases STRADα and
172 STARADβ (Baas et al., 2003). To determine whether Ulk4 regulates Stk36 enzymatic
173 activity, we carried out an *in vitro* kinase assay using GST-Gli2N, which contains the
174 Ulk3/Stk36 phosphorylation site S230, as substrate and either Fg-Stk36 or Fg-
175 Stk36/hUlk4-HA complex immunopurified from HEK293T cells as kinase. GST-Gli2N
176 containing S230A substitution was used as a negative control. As shown in Figure 3A,
177 Stk36 and Stk36/Ulk4 phosphorylated GST-Gli2N at similar levels and the
178 phosphorylation was abolished by the S230A mutation. This result suggests binding of
179 Ulk4 to Stk36 does not modulate Stk36 kinase activity.
180 We next determined whether Ulk4 is required for Stk36 kinase activation by Shh.
181 In *Drosophila*, Hh activates Fu by promoting its kinase domain dimerization and trans-
182 autophosphorylation on multiple S/T residues in its activation loop (AL) including T151,
183 T154, T158 and S159 (Shi et al., 2011; Zhang et al., 2011; Zhou and Kalderon, 2011).
184 Interestingly, the AL phosphorylation sites as well as the neighboring residues are
185 highly conserved between Fu and Stk36 (Figure. 3B) (Shi *et al.*, 2011), raising the
186 possibility that Stk36 could be activated by Shh through a similar mechanism. Indeed,
187 we found that Shh induced phosphorylation of Stk36 on T158/S159 in NIH-3T3 cells as
188 determined by a phospho-specific antibody that recognized pT158/pS159 (Figure. 3C)
189 (Shi *et al.*, 2011). To determine whether Shh-induced T158/S159 phosphorylation
190 depends on Stk36 kinase activity, we introduced either wild type Stk36 (CFP-Stk36^{WT})
191 or its kinase dead form (CFP-Stk36^{KR}) into NIH3T3 cells with endogenous Stk36 and

192 Ulk3 deleted (*Ulk3*^{KO} *Stk36*^{KO}) by CRISPR (Han *et al.*, 2019). As shown in Figure 3D,
193 Shh induced phosphorylation of CFP-Stk36^{WT} but not CFP-Stk36^{KR} on T158/S159,
194 suggesting that Shh promotes the phosphorylation of Stk36 AL via its kinase activity,
195 likely through trans-autophosphorylation as are the cases for other kinases. Hence,
196 phosphorylation of T158/S159 can be used as a readout for Stk36 kinase activation.
197 To determine whether AL phosphorylation promotes Stk36 kinase activation, we
198 converted both S151 and T154 to E (EE) to mimic phosphorylation or to A (AA) to block
199 phosphorylation on these sites (Figure 2B). We found that the phospho-mimetic
200 mutation (Stk36^{EE}) increased whereas phospho-deficient mutation (Stk36^{AA}) abolished
201 Stk36 kinase activity as determined by both Stk36 T158/S159 phosphorylation and Gli2
202 S230/S232 phosphorylation (Figure E-H), which is similar to what we have observed
203 previously for Fu (Shi *et al.*, 2011), suggesting that Hh stimulates kinase activation of
204 Stk36 and Fu through a similar mechanism.
205 To determine whether Ulk4 is required for Shh-induced Stk36 kinase activation,
206 we employed RNAi to deplete Ulk4 from NIH3T3 cells that express CFP-Stk36. As
207 shown in Figure 3I, depletion of Ulk4 did not affect Shh-induced phosphorylation of
208 CFP-Stk36 on T158/S159, suggesting that Ulk4 is not required for Stk36 kinase
209 activation in response to Shh stimulation.
210
211
212 **Ulk4 mediates the interaction between Stk36 and Gli2**
213
214
215 Another possible mechanism for Ulk4 to influence Gli2 phosphorylation by Stk36 is to
216 function as a scaffold that brings Stk36 and Gli2 into the same protein complex. Indeed,
217 we found that Ulk4 depletion diminished Stk36/Gli2 association in HEK293T cells

218 determined by Co-IP experiments (Figure 4A). By domain mapping, we found that the
219 kinase domain of Stk36 (Stk36N: aa1-260) but not its regulatory domain (Stk36C:
220 aa261-1351) interacted with Ulk4 (Figure 4B-C). Consistent with Ulk4 mediating the
221 interaction between Stk36 and Gli2, we found that Stk36N formed a complex with Gli2
222 more effectively than Stk36C (Figure 4D).

223 We next determined whether Ulk4 mediated Stk36/Gli2 interaction in NIH3T3
224 cells and whether this was regulated by Shh. NIH3T3 cells were infected with
225 lentiviruses expressing low levels of a Flag-tagged Stk36 (Fg-Stk36) and Myc-Gli2 and
226 treated with or without Shh. Co-IP experiments showed that Fg-Stk36 and Myc-Gli2
227 formed a complex regardless of Shh treatment (Figure 4E; lands 1-2). The interaction
228 between Fg-Stk36 and Myc-Gli2 was diminished by Ulk4 RNAi (Figure 4E; lands 3-4).
229 Reintroducing full-length hUlk4 (WT) but not hUlk4N or hUlk4C restored Fg-Stk36/Myc-
230 Gli2 association in Ulk4-depleted cells (Figure 4E; lands 5-10). Taken together, these
231 results suggest that Ulk4 functions as a molecular scaffold to bring Stk36 and Gli2 into
232 the same complex with its N-terminal region binding to Stk36 and its regulatory domain
233 interacting with Gli2 (Figure 4F).
234

235 **Shh stimulates ciliary tip accumulation of both Ulk4 and Stk36**
236
237 In response to Shh, Gli2 and Sufu accumulated at the tip of primary cilium in mammal
238 cells (Chen *et al.*, 2009; Haycraft *et al.*, 2005; Tukachinsky *et al.*, 2010), leading to the
239 general view that that Gli2 is converted to $Gli2^A$ at the ciliary tip (Goetz and Anderson,
240 2010; Jiang, 2021). Indeed, our previous study showed that Shh-stimulated Gli2
241 phosphorylation by Stk36/Ulk3 depended on ciliary localization of Gli2 (Han *et al.*, 2019).

242 These observations imply that Stk36/Ulk3 may translocate to the primary cilium to
243 phosphorylate Gli2 in response to Shh. To test this hypothesis, we treated NIH3T3 cells
244 stably expressing an N-terminal Myc-tagged Stk36 (Myc-Stk36) with or without Shh and
245 examined ciliary localization of Stk36 by immunostaining with an anti-Myc antibody.
246 Ciliary localization of endogenous Gli2 was examined by immunostaining with an anti-
247 Gli2 antibody. As shown in Figure 5A-B, Myc-Stk36 and Gli2 were barely detectable in
248 primary cilia in quiescent cells; however, Shh treatment induced ciliary tip localization of
249 both Myc-Stk36 and Gli2.
250 To determine whether Shh induced ciliary localization of Ulk4, NIH3T3 cells
251 stably expressing hUlk4-HA was treated with or without Shh, followed by
252 immunostaining with anti-HA and anti-Gli2 antibodies. Like Stk36, hUlk4-HA was barely
253 detectable in primary cilia in the absence of Shh but accumulated to the tips of primary
254 cilia colocalized with Gli2 after Shh stimulation (Figure 5C-D). We also examined
255 NIH3T3 cells simultaneously expressing Myc-Stk36 and hUlk4-HA and found that Shh
256 induced the ciliary tip co-localization of Ulk4 and Stk36 (Figure 5E-F). These results
257 suggest that Shh induced ciliary tip accumulation of Stk36-Ulk4-Gli2 protein complexes
258 to promote Gli2 phosphorylation and activation.
259
260 **Ulk4 and Stk36 depend on each other for their ciliary localization.**
261
262 As pseudokinases could regulate the subcellular localization of their interacting kinases,
263 we asked whether Ulk4 is required for ciliary localization of Stk36 in response to Shh.
264 NIH3T3 cells stabling expressing Myc-Stk36 were depleted of Ulk4 by shRNA and
265 treated with and without Shh. As shown in Figure 6A-B, Ulk4 RNAi diminished Shh-

266 induced ciliary tip localization of Myc-Stk36, suggesting that Ulk4 is required for ciliary
267 localization of Stk36 in response to Shh.
268 We next asked whether Ulk4 ciliary localization depends on Stk36. We first
269 determined the ciliary location of Ulk4 in NIH3T3 cells with both Stk36 and Ulk3
270 knocked out (DKO) by the CRISPR-Cas9 system (Han *et al.*, 2019). As shown in Figure
271 6C-D, Shh promoted ciliary tip enrichment of Ulk4-HA in the control cells but not in the
272 Stk36 and Ulk3 DKO cells. Adding back wild type Stk36 ($Stk36^{WT}$) but not its kinase
273 inactive form ($Stk36^{AA}$) restored Shh-induced Ulk4-HA ciliary tip accumulation in DKO
274 cells (Figure 6E-F). By contrast, neither wild type Ulk3 ($Ulk3^{WT}$) nor its kinase dead form
275 ($Ulk3^{KR}$) could rescue ciliary tip accumulation of Ulk4-HA in DKO cells (Figure 6E-F).
276 These results suggest that ciliary tip localization of Ulk4 depends on Stk36 kinase
277 activity.
278
279 **Ulk4 ciliary localization is regulated by its C-terminal phosphorylation**
280 Many pseudokinases are also the substrates of their interacting kinases (Kung and Jura,
281 2019). To determine whether Ulk4 is a Stk36 substrate and whether Stk36-mediated
282 phosphorylation of Ulk4 promotes its ciliary tip localization, we sought out to identify the
283 relevant phosphorylation sites. We generated several C-terminally HA-tagged truncated
284 forms of hUlk4 to narrow down the region essential for ciliary tip localization of Ulk4
285 (Figure 7A). These truncated forms were expressed in NIH3T3 cells in which
286 endogenous Ulk4 depleted by RNAi. Deleting the entire regulatory domain abolished
287 Shh-induced ciliary tip localization of the Ulk4 variant ($hUlk4_{1-450}$; Figure 7B-C). Deleting
288 the Stk36 binding region from Ulk4 ($hUlk4_{451-1275}$) also abolished its ciliary tip

289 localization in response to Shh, suggesting that binding to Stk36 is essential for Ulk4
290 ciliary localization. We generated two small deletions from the C-terminus of hUlk4
291 (hUlk4$_{1-1000}$ and hUlk4$_{1-1200}$; Figure 7A). Whereas hUlk4$_{1-1200}$ still localized to the ciliary
292 tip in response to Shh, hUlk4$_{1-1000}$ failed to do so (Figure 7B-C), suggesting that the
293 region between aa1000-1200 is essential for Shh-induced hUlk4 ciliary tip localization.
294 Within this region, T1021 and T1088/T1090 fall into the Fu/Ulk3/Stk36 phosphorylation
295 consensus site: S/T [X_5] E/D (Figure 7D) (Han *et al.*, 2019; Zhou and Jiang, 2022).
296 Furthermore, phosphorylation on T1021 can prime CK1-mediated phosphorylation on
297 T1023 as T1023 falls into the CK1 phosphorylation consensus site: D/E/$_{(p)}$S/$_{(P)}$T[X_{1-3}]
298 S/T (Knippschild et al., 2005).
299 To determine whether phosphorylation on these sites may regulate Ulk4 ciliary
300 localization, we generated hUlk4 variants carrying T1021A/1023A (hUlk4$^{T1021A/1023A}$) or
301 T1088A/T1090A (hUlk4$^{T1088A/T1090A}$) substitutions. These hUlk4 variants were expressed
302 in NIH3T3 cells with endogenous Ulk4 depleted by shRNA. We found that
303 hUlk4$^{T1088A/T1090A}$ but not hUlk4$^{T1021A/1023A}$ accumulated at ciliary tip in response to Shh
304 stimulation (Figure 7E-F), suggesting phosphorylation on T1021/1023 is essential for
305 Shh-induced ciliary tip localization of Ulk4.
306 To confirm T1021 phosphorylation by Stk36, we carried out an *in vitro* kinase
307 assay using immunopurified Fg-Stk36 as kinase and GST fusion protein containing
308 hUlk4 sequence from aa1017 to aa1036 (GST-hUlk4C) as substrate. As shown in
309 Figure 7G, immunopurified wild type Stk36 (Fg-Stk36^{WT}) but not its kinase inactive
310 variant (Fg-Stk36^{AA}) phosphorylated GST-hUlk4C. Mutating both T1021 and T1023 to A
311 (T1021A /T1023A) abolished the phosphorylation; however, mutating T1021A reduced

312 but not eliminated the phosphorylation, suggesting that in the absence of T1021
313 phosphorylation, T1023 could also be phosphorylated by Stk36. Interestingly, T1023 but
314 not T1021 is conserved in mouse Ulk4 (mUlk4) and mUlk4 contains an Ala at T1021
315 (Figure 7H), implying that phosphorylation of T1021 might be dispensable for Ulk4
316 function. Indeed, we found that mutating T1021 to A in hUlk4 (hUlk4^{T1021A}) did not affect
317 its ciliary tip accumulation in response to Shh (Figure 7E-F) as well as its activity in the
318 Hh pathway (see below).
319
320
321 **Ciliary localization of Ulk4 is essential for its function in Shh signaling**
322
323 To determine the importance of ciliary localization of Ulk4 for its function in Shh signal
324 transduction, we compared the Hh pathway related activity of ciliary localization
325 deficient hUlk4$^{T1021A/1023A}$ with that of ciliary localization competent hUlk4^{T1021A}
326 (equivalent to mUlk4^{WT}) and hUlk4^{WT} in NIH3T3 cells with endogenous Ulk4 depleted by
327 shRNA. We found that both hUlk4^{T1021A} and hUlk4^{WT} rescued Shh-induced ciliary tip
328 localization of coexpressed Myc-Stk36 (Figure 8A-B), phosphorylation of Myc-Gli2 at
329 S230/S232 (Figure 8C), and the expression of Shh target genes *Ptch1* and *Gli1* (Figure
330 8D-E). By contrast, hUlk4$^{T1021A/1023A}$ failed to rescue Shh-stimulated Stk36 ciliary tip
331 localization, Gli2 phosphorylation, as well as *Ptch1* and *Gli1* expression in Ulk4 depleted
332 cells (Figure 8A-E). These results suggest that ciliary localization of Ulk4 is essential for
333 its ability to promote Stk36 ciliary localization, Gli2 phosphorylation, and Hh pathway
334 activation (Figure 8F).
335

336 **Discussion**
337
338 The Gli family of transcription factors mediates the transcriptional output of the Hh
339 signaling pathway in species ranging from *Drosophila* to mammals but how Gli is
340 activated by Hh signaling is still poorly understood, especially in vertebrates where Gli
341 activation is thought to occur at the tip of primary cilium. We recently found that the
342 Fu/Ulk family kinases directly phosphorylate Ci and Gli2 on multiple sites to promote
343 their activation (Han *et al.*, 2019; Zhou *et al.*, 2022; Zhou and Jiang, 2022). In
344 mammalian cells, the Ulk family kinases Ulk3 and Stk36 (mammalian homolog of Fu)
345 act in parallel to promote Gli2 phosphorylation and activation in response to Shh. In
346 addition, Gli2 phosphorylation depends on its ciliary localization (Han *et al.*, 2019). In
347 this study, we found that Stk36 accumulated to the tip of primary cilium and colocalized
348 with Gli2 in response to Shh stimulation, consistent with Gli2 being converted into $Gli2^A$
349 at the ciliary tip. In addition, we identified another Ulk family member Ulk4, which is a
350 pseudokinase, as a mediator of Shh-induced Gli2 phosphorylation. We found that Ulk4
351 and Stk36 act in the same pathway but in parallel with Ulk3 to promote Gli2
352 phosphorylation and activation. The positive role of Ulk4 in Shh signaling could explain
353 why elevated expression of Ulk4 in certain genetic background could suppress the heart
354 outflow tract defects and holoprosencephaly caused by partially reduced Shh signaling
355 activity in LRP2-deficient mice (Mecklenburg *et al.*, 2021).
356 To determine the mechanism by which Ulk4 assists Stk36 to phosphorylate Gli2,
357 we explored whether Ulk4 regulated 1) the enzymatic activity of Stk36; 2) Shh-induced
358 Stk36 kinase activation; 3) the association of Stk36 and its substrate; and 4) ciliary
359 localization Stk36. In an *in vitro* kinase assay, we found that immunopurified Stk36

360 phosphorylated GST-Gli2N equally well regardless whether it interacted with Ulk4 or not,
361 suggesting that Ulk4 does not regulate Stk36 kinase activity. Rather, we found that Ulk4
362 is required for Stk36 to bind to its substrate Gli2. Ulk4 interacts with Stk36 through its N-
363 terminal region that contains the pseudokinase domain and with Gll2 via its C-terminal
364 regulatory domain. Depletion of Ulk4 diminished the physical association between Stk36
365 and Gli2. In further support the notion that Gli2 is brought to Stk36 through Ulk4, we
366 found that the kinase domain of Stk36, which binds Ulk4, also interacted with Gli2
367 whereas the C-terminal region interacted with neither Ulk4 nor Gli2.

368 Although Stk36/Ulk4/Gli2 complex formation appears to be constitutive
369 regardless the presence or absence of Shh, Stk36 kinase activation depends on Shh
370 stimulation. Like Fu, Stk36 is phosphorylated on multiple sites in the activation loop of
371 its kinase domain in response to Shh likely through trans-autophosphorylation, and
372 activation loop phosphorylation is essential for its kinase activation. Using a phospho-
373 specific antibody that recognized pT158/pS159 in the kinase activation loop of Fu/Stk36,
374 we found that Ulk4 depletion did not affect Shh-induced phosphorylation of Stk36 on
375 T158/S159, a readout for Stk36 kinase activation, suggesting that Ulk4 is dispensable
376 for Shh signaling to activate Stk36. In *Drosophila*, the kinesin-like protein Costal2 (Cos2)
377 mediates the activation of Fu kinase by Hh. Therefore, it would be interesting to
378 determine whether mammalian homologs Cos2, Kif7 and/or Kif27, participates in Stk36
379 kinase activation in response to Shh stimulation.

380 Hh signaling depends on primary cilia in vertebrates. Upon Shh stimulation, key
381 pathway components such as Smo and Gli proteins accumulate in primary cilia, and
382 Gli2 is accumulated to the ciliary tip and thought to be converted into its activator form

383 (Gli2^{A}) in this ciliary compartment. Consistent with this notion, we found that Shh
384 induced ciliary accumulation of both Ulk4 and Stk36 that colocalized with Gli2 at the
385 ciliary tip. Furthermore, we found that Ulk4 is required for ciliary tip accumulation of
386 Stk36. On the other hand, ciliary tip accumulation of Ulk4 depends on Stk36 kinase
387 activity and phosphorylation of its C-terminal region on T1023. Preventing Ulk4
388 phosphorylation on T1023 abolished ciliary tip accumulation of Ulk4, and its ability to
389 promote Stk36 ciliary tip accumulation, Gli2 phosphorylation and Hh pathway activation.
390 These results suggest that ciliary tip accumulation of Ulk4 is critical for its function in Hh
391 signal transduction, likely by increasing the local concentration of Stk36 and Gli2 to
392 promote effective phosphorylation of Gli2. It would be important to determine how
393 phosphorylation of T1023 promotes ciliary accumulation of Ulk4. A recent structure
394 study identified several motor proteins of the kinesin family (KIF1B, KIF3A, KIF3B, and
395 KAP3) as the interaction partners of Ulk4 (Preuss *et al.*, 2020). KIF3A, KIF3B and KAP3
396 are components of kinesin-2 motor that act in conjunction with intraflagellar transport
397 (IFT) complexes to transport cargoes into primary cilia (Goetz and Anderson, 2010). It
398 would be interesting to determine whether Ulk4 T1023 phosphorylation affects its
399 interaction with KIF3B, KAP3, or components in the IFT complexes.
400 Both Ulk4 and Stk36 have functions outside the Hh pathway. Stk36 is required
401 for motile ciliogenesis and its loss of function affects the construction of central pair
402 apparatus of “9+2” motile cilia in both zebrafish and mice (Nozawa et al., 2013; Wilson
403 *et al.*, 2009). Ulk4 malfunction also affects motile ciliogenesis of ependymal cells in
404 mutant mice, leading to hydrocephalus (Liu et al., 2016b; Vogel et al., 2012). A recent
405 study demonstrated that Ulk4 and Stk36 physically interact to mediate assembly of

406 motile flagella in the flagellated protist *Leishmania Mexicana* (McCoy et al., 2023).
407 However, the biochemical mechanism by which Ulk4/Stk36 regulates motile ciliogenesis
408 has remained unknown. Ulk4 could regulate Stk36 ciliary localization and/or kinase-
409 substrate interaction similar to what we have discovered for their role in Shh signaling.
410 The relevant substrates for Stk36 in motile ciliogenesis remain to be determined.
411 Knowing the phosphorylation consensus sites for the Fu/Ulk family kinase may facilitate
412 the identification of Stk36 substrates involved in the assembly of motile cilia and flagella.
413 Initially identified Fu/Ulk3/Stk36 phosphorylation sites in Ci/Gli and Cos2 fall into the
414 consensus: $S/T(X)_5D/E$, where the acidic residue at +6 position is essential (Han *et al.*,
415 2019; Zhou and Jiang, 2022). However, subsequent studies suggested that the spacing
416 between the phospho-acceptor site and the acid residue appears to be flexible. For
417 example, a Ulk3/Stk36 phosphorylation site in the C-terminal region of Gli2 has a
418 spacing of six residues between the phospho-acceptor site and the acid residue (Zhou
419 *et al.*, 2022). Here we found that a Stk36 phosphorylation site in the C-terminal region of
420 Ulk4 contains only four residues between the phospho-acceptor site and the acid
421 residue. Based on these findings, we propose an expanded consensus site for the
422 Fu/Ulk family kinases as $S/T(X)_{4\text{-}6}D/E$. It would be interesting to determine whether this
423 phosphorylation consensus sequence could be extended to other members of the Ulk
424 kinase family such as Ulk1/Atg1 and Ulk2, which are the initiating kinases for autophagy
425 (Zachari and Ganley, 2017).
426 Ulk4 has been implicated in several human diseases including hypertension and
427 psychiatric disorder such as schizophrenia (Luo *et al.*, 2022). Ulk4 also plays a role in
428 neurogenesis in mice by regulating neural stem cell pool and neurite branching

429 morphogenesis (Lang *et al.*, 2014; Lang *et al.*, 2016; Liu *et al.*, 2016a). In addition, Ulk4
430 regulates the integrity of white matter by promoting myelination (Liu *et al.*, 2018b). How
431 Ulk4 participates in these diverse processes has remained unclear. A recent study
432 revealed that Ulk4 binds several other kinases and phosphatases such as DAPK3,
433 LMTK2, PTPN14 as well as proteins implicated in the regulation of neuronal
434 differentiation and axonal regeneration including CAMSAP family proteins CAMSAP1/3
435 (Pongrakhananon et al., 2018; Preuss *et al.*, 2020). Given our findings regarding how
436 Ulk4 regulates Hh signaling, it is tempting to speculate that Ulk4 may also function as a
437 scaffold to bridge kinases or other enzymes to their substrates, or regulate the
438 subcellular localization of the interacting proteins in other biological processes.
439
440
441

442 **Materials and methods**

443

444 **DNA constructs**

445 Myc-Gli2 and GST-Gli2 were described previously (Han *et al.*, 2019). All GST-fusion
446 (the GST-tagged human Ulk4C^{WT}, Ulk4C^{T1021A}, Ulk4C$^{T1021A/1023A}$) proteins were
447 subcloned into the *pGEX 4T-1* vector using EcoRI and XhoI sites. N-terminally CFP-
448 tagged mouse Ulk3^{WT}, Ulk3^{KR}, N-terminally 6XMyc-tagged human Stk36, N-terminally
449 3XFg-tagged human Stk36^{WT}, Stk36^{AA} and the C-terminally 3XHA-tagged Human
450 Ulk4^{WT}, Ulk4$^{1-451}$, Ulk4$^{452-1275}$, Ulk4$^{1-1000}$, Ulk4$^{1-1200}$, Ulk4$^{T1021/1023A}$, Ulk4$^{T1088/1090A}$,
451 Ulk4^{T1021A} were subcloned into the *FUGW* vector with the EcoRI and BamHI sites. N-
452 terminally 3XFg-tagged human Stk36^{WT}, Stk36^{EE}, Stk36^{AA}, Stk36$^{1-260}$, Stk36$^{261-1315}$, and
453 C-terminally 3XHA-tagged Human Ulk4^{WT}, Ulk4$^{1-451}$, Ulk4$^{452-1275}$ were subcloned in the
454 *PLVX* vectors using the EcoRI and MluI sites. The Ulk4$^{T1021/1023A}$, Ulk4$^{T1088/1090A}$,
455 Ulk4^{T1021A}, Stk36^{EE}, Stk36^{AA}, were generated by PCR-mediated site-directed
456 mutagenesis.

457

458 **Cell culture, transfection, and lentiviral production**

459 NIH3T3 cells were cultured in Dulbecco's modified Eagle's medium (DMEM, Sigma)
460 containing10% bovine calf serum (Gibco) and 1% penicillin/streptomycin (Sigma). The
461 transfection was carried out by using the GenJet Plus *in vitro* DNA transfection kit
462 according to the manufacturer's instruction (SignaGen). HEK293T cells were cultured in
463 DMEM (Sigma) supplemented with 10% fetal bovine serum (Gibco) and 1%
464 penicillin/streptomycin (Sigma). PolyJet *in vitro* DNA transfection kit (SignaGen) was

465 used to do the transfection according to the manufacturer's instruction. Mouse
466 embryonic fibroblast cells (MEFs) were cultured in DMEM (Sigma) containing 10% FBS
467 (Gibco), and 1% streptomycin / penicillin (Sigma) according to the standard protocol.
468 For Shh-N treatment, cells were starved for 12 hours (0.5% BCS for NIH3T3 cells or 0.5%
469 FBS for MEF cells), recombinant human Shh N-terminal fragment (1 ng/ml; R&D
470 Systems, #8908-SH-005) was added to the medium for 12 hours or overnight.
471
472 **Immunostaining, immunoprecipitation, and western blotting analysis**
473 The protocol for Ulk4-HA/Myc-Stk36 immunostaining was carried out as previously
474 described (Han *et al.*, 2019). Immunofluorescence imaging was captured using a Zeiss
475 LSM700 laser scanning microscope. For ciliary Myc-Stk36/Ulk4-HA quantification, the
476 cilia were labelled with the acetylated-Tubulin and the Myc-Stk36/Ulk4-HA fluorescence
477 intensities were measured in the Myc-Stk36/Ulk4-HA image channel by ImageJ. Twenty
478 cells were randomly selected and calculated for each group. For immunoprecipitation
479 assay, after transfection for 48 hours, cells were washed twice with PBS and then lysed
480 on ice for 10 min with lysis buffer containing 1M Tris pH8.0, 5M NaCl, 1MNaF, 0.1M
481 Na3VO4, 1% CA630, 10% glycerol, and 0.5M EDTA (pH 8.0). Cell lysates were
482 incubated with protein A-Sepharose beads (Thermo scientific) for 1 hr at 4°C to
483 eliminate nonspecific binding proteins. After removal of the protein-A beads by
484 centrifugation, the cleared lysates were incubated with Myc (HA or Flag) antibody for 4
485 h or overnight. Protein complexes were collected by incubation with protein A-
486 Sepharose beads for 1 hr at 4°C, followed by centrifugation. Immunoprecipitates were
487 washed three times for 5 min each with lysis buffer and were separated on SDS-PAGE.

488 Western blot was carried out using standard protocol. Antibodies used in this study
489 were as follows: Mouse anti-Myc (Santa Cruz Biotechnology; 9E10), Mouse anti-Flag
490 (Sigma; M2), Mouse anti-HA (Santa Cruz Biotechnology; F7), Mouse anti-acetylated
491 Tubulin (sigma; T7451; staining:1:1000), Rabbit anti-Myc (abcam; ab9106; staining
492 1:2000), Rabbit anti-HA (AbCam; ab9110; staining 1:500), Goat anti-Gli2 (R&D system;
493 AF3635; staining 1:1000).

494

495 ***In vitro* kinase assay**

496 *In vitro* kinase assay was performed by incubating 25 μL of reaction mixtures containing
497 150 mM Tris-HCl (pH 7.5), 0.2 mM Mg2+/ATP, 1 μg of purified GST-Ulk4/Gli2 fusion
498 proteins, together with appropriate amount of kinase for 30mins at 30°C. The reaction
499 was terminated by adding 2× SDS loading buffer. The resultant samples were load on
500 SDS-PAGE and subjected to pIMAGO phospho-protein detection kit with fluor-680
501 (Sigma) detection kit and LI-COR Odyssey platform for western blot analyses of
502 phosphorylated proteins (Millipore Sigma). Fg-Stk36^{WT} and Fg-Stk36^{AA} were
503 immunopurified from HEK293 cells transfected with the Fg-Stk36^{WT} or Fg-Stk36^{AA}
504 construct.

505

506 **Viral Infection and shRNA**

507 For lentivirus generation, *pLKO.1* vectors expressing shRNA or *FUGW* vectors
508 expressing transgenes were co-transfected with package vectors (PSPAX2 and
509 PMDG2) into HEK293T cells using PolyJet (SignaGen). The supernatants were

510 collected after 48 h and 72 h transfection, filtered through a 0.45 mM filter and
511 centrifuged at 20,000 g for 2 h. The sediment containing the viruses was re-suspended,
512 aliquoted in small volume of culture medium and stored at -80°C for future use. For cell
513 infection, lentiviruses were added to 70% confluent wild type NIH3T3 or MEF cells
514 together with Polybrene (Sigma, Cat. No. H9268) for overnight to make the stable
515 NIH3T3 or MEF cell lines expressing transgene or shRNA . The Mouse Ulk4 shRNA
516 lentiviral vector was purchased from Sigma (TRCN0000328628). The Non-Target
517 shRNA Plasmid DNA (sigma; SHC016) was used as control.

518

519 **RNA interference using siRNAs**

520 For RNAi experiments in NIH3T3 or MEF cells, the siRNAs were purchased from Sigma.
521 The sequences for Ulk3 silencing were: 5'-GUGUACAAGGCCUACGCCA-3' (Cat#
522 SASI_ Mm02 _ 00444409) and 5'-CUGAGAAGGUGGCCCGUGU-3' (Cat#
523 SASI_Mm02_00444410). The sequences for Stk36 silencing were: 5'-
524 GGUAUACUGGCUUCAGAAA-3' (Cat# SASI_ Mm02 _00345637) and 5'-
525 GCCUUAUGUGCUUUGCUGU-3' (Cat# SASI_Mm01_00167751). The
526 sequences for negative control were: 5'-UUCUCCGAACGUGUCACG U-3'. The RNAi
527 MAX reagent (Invitrogen Cat. No. 13778150) was used for the transfection of siRNA.
528 The knockdown efficiency was validated via real-time PCR.

529

530 **Quantitative RT-PCR**

531 Total RNA was extracted from 1 × 10^6 cells using the RNeasy Plus Mini Kit (Qiagen),
532 and cDNA was synthesized with High-Capacity cDNA Reverse Transcription Kit
533 (Applied Biosystems; 01279158) and qPCR was performed using Fast SYBR Green
534 Master Mix (Applied Biosystems; 2608088) and a Bio-Rad CFX96 real-time PCR
535 system (BIO-RAD; HSP9601). The RT-qPCR was performed in triplicate for each of
536 three independent biological replicates. Quantification of mRNA levels was calculated
537 using the comparative CT method. Primers: Gli1, 5'-GTGCACGTTTGAAGGCTGTC-3'
538 and 5'-GAGTGGGTCCGATTCTGGTG-3'; Ptch1, 5'-GAAGCCACAGAAAACCCTGTC-3'
539 and 5'-GCCGCAAGCCTTCTCTACG-3'; Ulk3, 5'- ACGAAACATCTCTCACTTG-3' and
540 5'- TGCTGGGCAAAGCCAAAGTC-3'; Ulk4, 5'- ATGCAGAGTGTGATTGCGTTG-3' and
541 5'- GAGTGGCAGTTTCTGTGAACA-3'; Stk36, 5'- CGCATCCTACACCGAGATATGA-3'
542 and 5'- AAATCCAAAGTCACAGAGCTTGA-3';GAPDH, 5'-
543 GTGGTGAAGCAGGCATCTGA-3' and 5'-GCCATGTAGGCCATGAGGTC-3'.
544

545 **Acknowledgements**

546 We thank Bing Wang, Xu Li, and Yong Cho for technical assistance, Pancheng Xie and
547 Yi Liu for reagents. J. Jiang is a Eugene McDermott Endowed Scholar in Biomedical
548 Science at the University of Texas Southwestern.

549
550 **Declaration of interests**
551
552 The authors declare no competing interests.

553 **Reference**

554 Arveseth, C.D., Happ, J.T., Hedeen, D.S., Zhu, J.F., Capener, J.L., Klatt Shaw, D.,
555 Deshpande, I., Liang, J., Xu, J., Stubben, S.L., et al. (2021). Smoothened transduces
556 Hedgehog signals via activity-dependent sequestration of PKA catalytic subunits. PLoS
557 biology *19*, e3001191. 10.1371/journal.pbio.3001191.
558 Baas, A.F., Boudeau, J., Sapkota, G.P., Smit, L., Medema, R., Morrice, N.A., Alessi,
559 D.R., and Clevers, H.C. (2003). Activation of the tumour suppressor kinase LKB1 by the
560 STE20-like pseudokinase STRAD. Embo Journal. *22*, 3062-3072.
561 10.1093/emboj/cdg292.
562 Briscoe, J., and Therond, P.P. (2013). The mechanisms of Hedgehog signalling and its
563 roles in development and disease. Nat Rev Mol Cell Biol *14*, 418-431. 10.1038/nrm3598.
564 Chen, M.H., Wilson, C.W., Li, Y.J., Law, K.K., Lu, C.S., Gacayan, R., Zhang, X., Hui,
565 C.C., and Chuang, P.T. (2009). Cilium-independent regulation of Gli protein function by
566 Sufu in Hedgehog signaling is evolutionarily conserved. Genes Dev *23*, 1910-1928.
567 23/16/1910 [pii]
568 10.1101/gad.1794109.
569 Chen, Y., and Jiang, J. (2013). Decoding the phosphorylation code in Hedgehog signal
570 transduction. Cell Res *23*, 186-200. 10.1038/cr.2013.10.
571 Chen, Y., Sasai, N., Ma, G., Yue, T., Jia, J., Briscoe, J., and Jiang, J. (2011). Sonic
572 Hedgehog dependent phosphorylation by CK1alpha and GRK2 is required for ciliary
573 accumulation and activation of smoothened. PLoS biology *9*, e1001083.
574 10.1371/journal.pbio.1001083.

575 Cooper, A.F., Yu, K.P., Brueckner, M., Brailey, L.L., Johnson, L., McGrath, J.M., and
576 Bale, A.E. (2005). Cardiac and CNS defects in a mouse with targeted disruption of
577 suppressor of fused. Development *132*, 4407-4417.
578 Corbit, K.C., Aanstad, P., Singla, V., Norman, A.R., Stainier, D.Y., and Reiter, J.F.
579 (2005). Vertebrate Smoothened functions at the primary cilium. Nature. *437*, 1018-1021.
580 Dunaeva, M., Michelson, P., Kogerman, P., and Toftgard, R. (2003). Characterization of
581 the physical interaction of Gli proteins with SUFU proteins. J Biol Chem *278*, 5116-5122.
582 10.1074/jbc.M209492200.
583 Goetz, S.C., and Anderson, K.V. (2010). The primary cilium: a signalling centre during
584 vertebrate development. Nat Rev Genet *11*, 331-344. nrg2774 [pii]
585 10.1038/nrg2774.
586 Han, Y., and Jiang, J. (2021). Expression and purification of fused kinase from insect
587 cells for in vitro kinase assay. STAR Protoc *2*, 100376. 10.1016/j.xpro.2021.100376.
588 Han, Y., Shi, Q., and Jiang, J. (2015). Multisite interaction with Sufu regulates Ci/Gli
589 activity through distinct mechanisms in Hh signal transduction. Proc Natl Acad Sci U S
590 A *112*, 6383-6388. 10.1073/pnas.1421628112.
591 Han, Y., Wang, B., Cho, Y.S., Zhu, J., Wu, J., Chen, Y., and Jiang, J. (2019).
592 Phosphorylation of Ci/Gli by Fused Family Kinases Promotes Hedgehog Signaling. Dev
593 Cell *50*, 610-626 e614. 10.1016/j.devcel.2019.06.008.
594 Haycraft, C.J., Banizs, B., Aydin-Son, Y., Zhang, Q., Michaud, E.J., and Yoder, B.K.
595 (2005). Gli2 and gli3 localize to cilia and require the intraflagellar transport protein
596 polaris for processing and function. PLoS Genet *1*, e53.

597 Jacobsen, A.V., and Murphy, J.M. (2017). The secret life of kinases: insights into non-
598 catalytic signalling functions from pseudokinases. Biochemical Society transactions *45*,
599 665-681. 10.1042/BST20160331.
600 Jiang, J. (2002). Degrading Ci: who is Cul-pable? Genes & Dev *16*, 2315-2321.
601 Jiang, J. (2021). Hedgehog signaling mechanism and role in cancer. Semin Cancer Biol.
602 10.1016/j.semcancer.2021.04.003.
603 Jiang, J., and Hui, C.C. (2008). Hedgehog signaling in development and cancer. Dev
604 Cell *15*, 801-812.
605 Kim, J., Kato, M., and Beachy, P.A. (2009). Gli2 trafficking links Hedgehog-dependent
606 activation of Smoothened in the primary cilium to transcriptional activation in the
607 nucleus. Proc Natl Acad Sci U S A *106*, 21666-21671. 10.1073/pnas.0912180106.
608 Knippschild, U., Gocht, A., Wolff, S., Huber, N., Lohler, J., and Stoter, M. (2005). The
609 casein kinase 1 family: participation in multiple cellular processes in eukaryotes. Cellular
610 signalling *17*, 675-689. S0898-6568(04)00297-9 [pii]
611 10.1016/j.cellsig.2004.12.011.
612 Kung, J.E., and Jura, N. (2019). Prospects for pharmacological targeting of
613 pseudokinases. Nat Rev Drug Discov *18*, 501-526. 10.1038/s41573-019-0018-3.
614 Lang, B., Pu, J., Hunter, I., Liu, M., Martin-Granados, C., Reilly, T.J., Gao, G.D., Guan,
615 Z.L., Li, W.D., Shi, Y.Y., et al. (2014). Recurrent deletions of ULK4 in schizophrenia: a
616 gene crucial for neuritogenesis and neuronal motility. J Cell Sci *127*, 630-640.
617 10.1242/jcs.137604.
618 Lang, B., Zhang, L., Jiang, G., Hu, L., Lan, W., Zhao, L., Hunter, I., Pruski, M., Song,
619 N.N., Huang, Y., et al. (2016). Control of cortex development by ULK4, a rare risk gene

620 for mental disorders including schizophrenia. Scientific reports *6*, 31126.
621 10.1038/srep31126.
622 Liu, M., Fitzgibbon, M., Wang, Y., Reilly, J., Qian, X., O'Brien, T., Clapcote, S., Shen, S.,
623 and Roche, M. (2018a). Ulk4 regulates GABAergic signaling and anxiety-related
624 behavior. Transl Psychiatry *8*, 43. 10.1038/s41398-017-0091-5.
625 Liu, M., Guan, Z., Shen, Q., Flinter, F., Dominguez, L., Ahn, J.W., Collier, D.A., O'Brien,
626 T., and Shen, S. (2016a). Ulk4 Regulates Neural Stem Cell Pool. Stem Cells *34*, 2318-
627 2331. 10.1002/stem.2423.
628 Liu, M., Guan, Z., Shen, Q., Lalor, P., Fitzgerald, U., O'Brien, T., Dockery, P., and Shen,
629 S. (2016b). Ulk4 Is Essential for Ciliogenesis and CSF Flow. J Neurosci *36*, 7589-7600.
630 10.1523/JNEUROSCI.0621-16.2016.
631 Liu, M., Xu, P., Guan, Z., Qian, X., Dockery, P., Fitzgerald, U., O'Brien, T., and Shen, S.
632 (2018b). Ulk4 deficiency leads to hypomyelination in mice. Glia *66*, 175-190.
633 10.1002/glia.23236.
634 Luo, S., Zheng, N., and Lang, B. (2022). ULK4 in Neurodevelopmental and
635 Neuropsychiatric Disorders. Front Cell Dev Biol *10*, 873706. 10.3389/fcell.2022.873706.
636 McCoy, C.J., Paupelin-Vaucelle, H., Gorilak, P., Beneke, T., Varga, V., and Gluenz, E.
637 (2023). ULK4 and Fused/STK36 interact to mediate assembly of a motile flagellum. Mol
638 Biol Cell, mbcE22060222. 10.1091/mbc.E22-06-0222.
639 Mecklenburg, N., Kowalczyk, I., Witte, F., Gorne, J., Laier, A., Mamo, T.M., Gonschior,
640 H., Lehmann, M., Richter, M., Sporbert, A., et al. (2021). Identification of disease-
641 relevant modulators of the SHH pathway in the developing brain. Development *148*.
642 10.1242/dev.199307.

643 Murone, M., Luoh, S.M., Stone, D., Li, W., Gurney, A., Armanini, M., Grey, C.,
644 Rosenthal, A., and de Sauvage, F.J. (2000). Gli regulation by the opposing activities of
645 fused and suppressor of fused. Nat Cell Biol *2*, 310-312.
646 Nozawa, Y.I., Yao, E., Lin, C., Yang, J.H., Wilson, C.W., Gacayan, R., and Chuang, P.T.
647 (2013). Fused (Stk36) is a ciliary protein required for central pair assembly and motile
648 cilia orientation in the mammalian oviduct. Dev Dyn *242*, 1307-1319.
649 10.1002/dvdy.24024.
650 Pongrakhananon, V., Saito, H., Hiver, S., Abe, T., Shioi, G., Meng, W., and Takeichi, M.
651 (2018). CAMSAP3 maintains neuronal polarity through regulation of microtubule stability.
652 Proceedings of the National Academy of Sciences *115*, 9750-9755.
653 doi:10.1073/pnas.1803875115.
654 Preuss, F., Chatterjee, D., Mathea, S., Shrestha, S., St-Germain, J., Saha, M., Kannan,
655 N., Raught, B., Rottapel, R., and Knapp, S. (2020). Nucleotide Binding, Evolutionary
656 Insights, and Interaction Partners of the Pseudokinase Unc-51-like Kinase 4. Structure
657 *28*, 1184-1196 e1186. 10.1016/j.str.2020.07.016.
658 Rohatgi, R., Milenkovic, L., and Scott, M.P. (2007). Patched1 regulates hedgehog
659 signaling at the primary cilium. Science *317*, 372-376.
660 Shi, Q., Li, S., Jia, J., and Jiang, J. (2011). The Hedgehog-induced Smoothened
661 conformational switch assembles a signaling complex that activates Fused by
662 promoting its dimerization and phosphorylation. Development *138*, 4219-4231.
663 dev.067959 [pii]
664 10.1242/dev.067959.

665 Tempe, D., Casas, M., Karaz, S., Blanchet-Tournier, M.F., and Concordet, J.P. (2006).
666 Multisite protein kinase A and glycogen synthase kinase 3beta phosphorylation leads to
667 Gli3 ubiquitination by SCFbetaTrCP. Mol Cell Biol *26*, 4316-4326.
668 Tukachinsky, H., Lopez, L.V., and Salic, A. (2010). A mechanism for vertebrate
669 Hedgehog signaling: recruitment to cilia and dissociation of SuFu-Gli protein complexes.
670 Journal Of Cell Biology. *191*, 415-428. jcb.201004108 [pii]
671 10.1083/jcb.201004108.
672 Villavicencio, E.H., Walterhouse, D.O., and Iannaccone, P.M. (2000). The sonic
673 hedgehog-patched-gli pathway in human development and disease. Am J Hum Genet
674 *67*, 1047-1054.
675 Vogel, P., Read, R.W., Hansen, G.M., Payne, B.J., Small, D., Sands, A.T., and
676 Zambrowicz, B.P. (2012). Congenital hydrocephalus in genetically engineered mice. Vet
677 Pathol *49*, 166-181. 10.1177/0300985811415708.
678 Wang, B., Fallon, J.F., and Beachy, P.A. (2000). Hedgehog-regulated processing of
679 Gli3 produces an anterior/posterior repressor gradient in the developing vertebrate limb.
680 Cell *100*, 423-434.
681 Wang, B., and Li, Y. (2006). Evidence for the direct involvement of {beta}TrCP in Gli3
682 protein processing. Proc Natl Acad Sci U S A *103*, 33-38.
683 Wilson, C.W., Nguyen, C.T., Chen, M.H., Yang, J.H., Gacayan, R., Huang, J., Chen,
684 J.N., and Chuang, P.T. (2009). Fused has evolved divergent roles in vertebrate
685 Hedgehog signalling and motile ciliogenesis. Nature. *459*, 98-102. nature07883 [pii]
686 10.1038/nature07883.

687 Zachari, M., and Ganley, I.G. (2017). The mammalian ULK1 complex and autophagy
688 initiation. Essays Biochem *61*, 585-596. 10.1042/EBC20170021.
689 Zhang, Y., Mao, F., Lu, Y., Wu, W., Zhang, L., and Zhao, Y. (2011). Transduction of the
690 Hedgehog signal through the dimerization of Fused and the nuclear translocation of
691 Cubitus interruptus. Cell Res *21*, 1436-1451. 10.1038/cr.2011.136.
692 Zhou, M., Han, Y., Wang, B., Cho, Y.S., and Jiang, J. (2022). Dose-dependent
693 phosphorylation and activation of Hh pathway transcription factors. Life Sci Alliance *5*.
694 10.26508/lsa.202201570.
695 Zhou, M., and Jiang, J. (2022). Gli Phosphorylation Code in Hedgehog Signal
696 Transduction. Front Cell Dev Biol *10*, 846927. 10.3389/fcell.2022.846927.
697 Zhou, Q., and Kalderon, D. (2011). Hedgehog Activates Fused through Phosphorylation
698 to Elicit a Full Spectrum of Pathway Responses. Dev Cell *20*, 802-814. S1534-
699 5807(11)00174-2 [pii]
700 10.1016/j.devcel.2011.04.020.
701
702
703

704 **Figure legend**
705
706

707 **Figure 1. Ulk4 acts in conjunction with Stk36 to promote Shh-mediated Gli**

708 **activation**

709 (A-B) Relative *Gli1* (A) and *Ptch1* (B) mRNA levels measured by RT-qPCR in NIH3T3

710 cells expressing the indicated shRNA and a human Ulk4 (hUlk4) lentiviral construct and

711 treated with or without Shh-N.

712 (C-D) Relative *Ptch1* mRNA levels measured by RT-qPCR in NIH3T3 cells treated with

713 the indicated RNAi and with or without Shh-N.

714 (E) Western blot analysis of Myc-Gli2 phosphorylation in NIH3T3 cells expressing the

715 indicated shRNA and hUlk4 lentiviral construct and treated with or without Shh-N.

716 (F-G) Western blot analysis of Myc-Gli2 phosphorylation in NIH3T3 cells with the

717 indicated RNAi in the presence or absence of Shh-N treatment.

718 (H) Schematic diagram showing the functional relationship among Ulk4, Stk36 and Ulk3

719 in Shh-induced Gli activation.

720 Data are mean ± SD from three independent experiments. ***$p < 0.001$ (Student's t test).

721 NS: not significant.

722

723 **Figure 2. Ulk4 forms a complex with Stk36 and Gli2**

724 (A) Ulk4 forms a complex with Stk36. HEK293T cells were transfected with hUlk4-HA

725 and CFP-Stk36 constructs, followed by Co-IP and western blot analyses with the

726 indicated antibodies.

727 (B) Ulk4 forms a complex with Gli2 and Sufu. HEK293T cells were transfected with
728 hUlk4-HA, Myc-Gli2 and Fg-Sufu constructs, followed by Co-IP and western blot
729 analyses with the indicated antibodies.
730 (C) Ulk4 domain structure and deletion mutants used for Co-IP experiments.
731 (D-E) Ulk4 interacted with Stk36 through its N-terminal domain (D) and with Myc-
732 Gli2/Fg-Sufu through its C-terminal region (E). HEK293T cells were transfected with the
733 indicated hUlk4, Fg-Stk36, Myc-Gli2 and Fg-Sufu constructs, followed by Co-IP and
734 western blot analyses.
735
736 **Figure 3. Ulk4 is dispensable for Stk36 kinase activation.**
737
738 (A) *In vitro* kinase assay using the immunopurified Fg-Stk36 or Fg-Stk36/hUlk4-HA as
739 kinase and GST-Gli2N^{WT} or GST-Gli2N^{S230A} as substrate. pIMAGO was used to detect
740 GST-Gli2N phosphorylation. The levels of Fg-Stk36/hUlk4-HA and GST/GST-Gli2N
741 were analyzed by western blot and coomassie blue (CB) staining, respectively.
742 (B) The schematic diagram showing the sequence alignment of the activation segments
743 of *Drosophila* Fu, mouse Stk36 (mStk36) and human Stk36 (hStk36). The conserved
744 Ser/Thr residues in the activation loop are color-coded in green. The residues used as
745 antigen for developing pT158/pS159 are colored in yellow. Amino acid substitutions for
746 Stk36 variants are indicated.
747 (C) Shh induced Stk36 phosphorylation on T158/S159. NIH3T3 cells expressing CFP-
748 Stk36 lentiviral construct were treated with or without Shh-N, followed by
749 IP with an GFP antibody and western blot analysis using an antibody against the
750 phosphorylated T158/S159 (pT158/pS159).

751 (D) Shh induced Stk36 phosphorylation on T158/S159 depending on Stk36 kinase
752 activity. Ulk3 and Stk36 double knockout NIH3T3 cells expressing CFP-Stk36^{WT} or
753 CFP-Stk36^{KR} (kinase dead) lentiviral construct were treated with or without Shh-N,
754 followed by IP with an GFP antibody and western blot analysis with the pT158/pS159
755 antibody.
756 (E-F) Western blot analysis (E) and quantification (F) of T158/S159 phosphorylation in
757 Fg-Stk36^{WT}, Fg-Stk36^{EE} or Fg-Stk36^{AA}. HEK293T cells were transfected with the
758 indicated Fg-Stk36 constructs, followed by IP with anti-Flag antibody and western blot
759 analysis with the indicated antibodies.
760 (G-H) Western blot analysis (G) and quantification (H) of Myc-Gli2 phosphorylation on
761 S230/S232 by the wild type (WT) or indicated Stk36 variants in HEK293T cells.
762 (I) Ulk4 is not required for Shh-induced Stk36 kinase activation. NIH3T3 cells
763 expressing the indicated shRNA and CFP-Stk36 lentiviral construct were treated with or
764 without Shh-N, followed by IP with an GFP antibody and western blot analysis with the
765 pT158/pS159 antibody (right). The knockdown efficiency of Ulk4 was determined by RT-
766 qPCR (left).
767 Data are mean ± SD from three independent experiments. **$p < 0.01$, and ***$p < 0.001$
768 (Student's t test).
769
770 **Figure 4. Ulk4 mediates the interaction between Stk36 and Gli2.**
771
772 (A) Depletion of Ulk4 diminished the association between Stk36 and Gli2. HEK293T
773 cells were transfected with the indicated shRNA and Fg-Stk36 and Myc-Gli2 constructs,
774 followed by CoIP and western blot analysis with the indicated antibodies.

775 (B) Domain structure and deletion mutants of human Stk36 used for the Co-IP
776 experiments.
777 (C-D) Stk36 binds to Ulk4 and Gli2 through its N-terminal kinase domain. HEK293T
778 cells were transfected with Ulk4-HA (C) or Myc-Gli2 (D) and the indicated Fg-Stk36
779 constructs, followed by Co-IP and western blot analyses with the indicated antibodies.
780 (E) Both N- and C-terminal domains of Ulk4 are required for mediating Stk36/Gli2
781 association. NIH3T3 cell lines stably expressing control (Ctrl) or Ulk4 shRNA were
782 infected with lentiviruses expressing the indicated hUlk4 constructs (diagrams shown on
783 F, right), Fg-Stk36 and Myc-Gli2, and treated with or without the Shh-N, followed by
784 CoIP and western blot analysis with the indicated antibodies.
785 (F) Schematic diagram showing the interaction relationship between Ulk4 and Stk36,
786 Gli2.
787
788 **Figure 5. Shh stimulates ciliary tip accumulation of both Ulk4 and Stk36.**
789
790 (A-D) Representative images of immunostaining (A, C) and quantification (B, D) of
791 ciliary tip localized Myc-Stk36 (green in A) or Ulk4-HA (green in C) and Gli2 (blue in A
792 and C) in NIH3T3 cells infected with the Myc-Stk36 or Ulk4-HA lentivirus and treated
793 with or without Shh-N. Primary cilia were marked by acetylated tubulin (Ac-tub) staining
794 (red in A and C).
795 (E-F) Representative images of immunostaining (E) and quantification (F) of ciliary tip
796 localized Myc-Stk36 (green) and Ulk4-HA (blue) in NIH3T3 cells co-infected with Myc-
797 Stk36 and Ulk4-HA lentiviruses and treated with or without Shh-N. Primary cilia were
798 marked by Ac-Tub staining (red).

799 The intensity of ciliary-localized WT and mutant Ulk4-HA was measured by Image J. 20
800 cells were randomly selected and counted for each group. Data are mean ± SD from
801 three independent experiments. ***p < 0.001 (Student's t test). Scale bars are 5 μM.
802
803 **Figure 6. Stk36 and Ulk4 depend on each other for their ciliary tip accumulation**
804 (A-B) Representative images of immunostaining (A) and quantification (B) of ciliary tip
805 localized Myc-Stk36 in NIH3T3 cells infected with the indicated shRNA and Myc-Stk36
806 lentivirus in the presence or absence of Shh-N. Primary cilia were marked by Ac-Tub
807 staining (red); Myc-Stk36 was marked by Myc staining (green); nuclei were marked by
808 DAPI (Blue).
809 (C-D) Representative images of immunostaining (C) and quantification (D) of ciliary tip
810 localized Ulk4-HA (green) in wild type (Ctrl) or Ulk3 and Stk36 double knockout (DKO)
811 NIH3T3 cells treated with or without Shh-N. Primary cilia were marked by Ac-Tub
812 staining (red) and nuclei by DAPI (Blue).
813 (E-F) Representative images of immunostaining (E) and quantification (F) of ciliary-
814 localized Ulk4-HA (green) in Shh-N treated control or DKO NIH3T3 cells infected with or
815 without lentiviruses expressing the indicated Ulk3 or Stk36 constructs.
816 The intensity of ciliary-localized Myc-Stk36 or WT and mutant Ulk4-HA was measured
817 by Image J. 20 cells were randomly selected and counted for each group. Data are
818 mean ± SD from three independent experiments. ***p < 0.001 (Student's t test). Scale
819 bars are 5 μM.
820

821 **Figure 7. Ulk4 ciliary tip accumulation is promoted by its phosphorylation by**

822 **Stk36**

823 (A) Diagrams of hUlk4 deletion constructs.

824 (B-C) Representative images of immunostaining (B) and quantification (C) of ciliary tip

825 localized full-length or truncated hUlk4-HA in Ulk4 knockdown cells treated with Shh-N.

826 (D) Stk36 and CK1 phosphorylation sites in the C-terminal region of hUlk4.

827 (E-F) Representative images of immunostaining (E) and quantification (F) of ciliary tip

828 localized wild type (WT) or mutant hUlk4-HA baring the indicated amino acid

829 substitutions in Ulk4 knockdown NIH3T3 cells treated with Shh-N.

830 (G) *In vitro* kinase assay using the immunopurified Fg-Stk36^{WT} or Fg-Stk36^{AA} as kinase

831 and the indicated GST-Ulk4C fusion proteins as substrates. Phosphorylation was

832 detected by the pIMAGO system.

833 (H) Schematic diagram showing the sequence alignment of C-terminal phosphorylation

834 sites of mouse Ulk4 (mUlk4) and human Ulk4 (hUlk4). The Thr residues phosphorylated

835 by Stk36 are color-coded in green.

836 The intensity of ciliary-localized WT and mutant Ulk4-HA was measured by Image J. 20

837 cells were randomly selected and counted for each group. Data are mean ± SD from

838 three independent experiments. ***$p < 0.001$ (Student's t test). Scale bars are 5 μM.

839

840 **Figure 8. Ciliary tip localization of Ulk4 is required for Shh signal transduction**

841

842 (A-B) Representative images of immunostaining (A) and quantification (B) of ciliary tip

843 localized Myc-Stk36 and hUlk4 in Ulk4-depleted NIH3T3 cells expressing the indicated

844 hUlk4 constructs and treated with Shh.

845 (C) Western blot analysis of Myc-Gli2 phosphorylation on S230/S232 in NIH3T3 cells
846 expressing the indicated shRNA and hUlk4 lentiviral constructs and treated with or
847 without Shh-N.
848 (D-E) Relative *Gli1* (D) and *Ptch1* (E) mRNA levels in NIH3T3 cells expressing the
849 indicated shRNA and hUlk4 lentiviral constructs treated with or without Shh-N.
850 (F) Model for how Ulk4 participates in Shh signaling. See text for details.
851 The intensity of ciliary-localized proteins was measured by Image J. 20 cells were
852 randomly selected and counted for each group. Data are mean ± SD from three
853 independent experiments. ***$p < 0.001$ (Student's t test). Scale bars are 5 μM.
854

855

856 **Supplementary Figure legends**
857

858 **Figure 1- figure supplement 1. The knockdown efficiency of Ulk4, Ulk3 and Stk36**
859 **in NIH3T3 cells.**
860 (A-C) Relative Ulk4 (A), Ulk3 (B), and Stk36 (C) mRNA levels measured by RT-qPCR in
861 NIH3T3 cells treated with the indicated shRNA or siRNA.
862 Data are mean ± SD from three independent experiments. ***$p< 0.001$ (Student's t test).
863

864 **Figure 1- figure supplement 2. Ulk4 acts in conjunction with Stk36 to regulate**
865 **Shh-induced expression of *Gli1* and *Ptch1* in MEFs.**
866 (A-B) Relative *Gli1* (A) and *Ptch1* (B) mRNA levels measured by RT-qPCR in MEF cells
867 expressing the indicated shRNA and hUlk4 lentiviral constructs with or without Shh-N
868 treatment.

869 (C-D) Relative *Gli1* mRNA levels measured by RT-qPCR in MEF cells with the indicated

870 RNAi knockdown in the presence or absence of Shh-N treatment.

871 (E) Relative Ulk4, Ulk3 and Stk36 mRNA levels measured by RT-qPCR in MEF cells

872 treated with the indicated shRNA or siRNA.

873 Data are mean ± SD from three independent experiments. ***$p < 0.001$ (Student's t test).

874
875
876
877
878
879
880
881
882
883

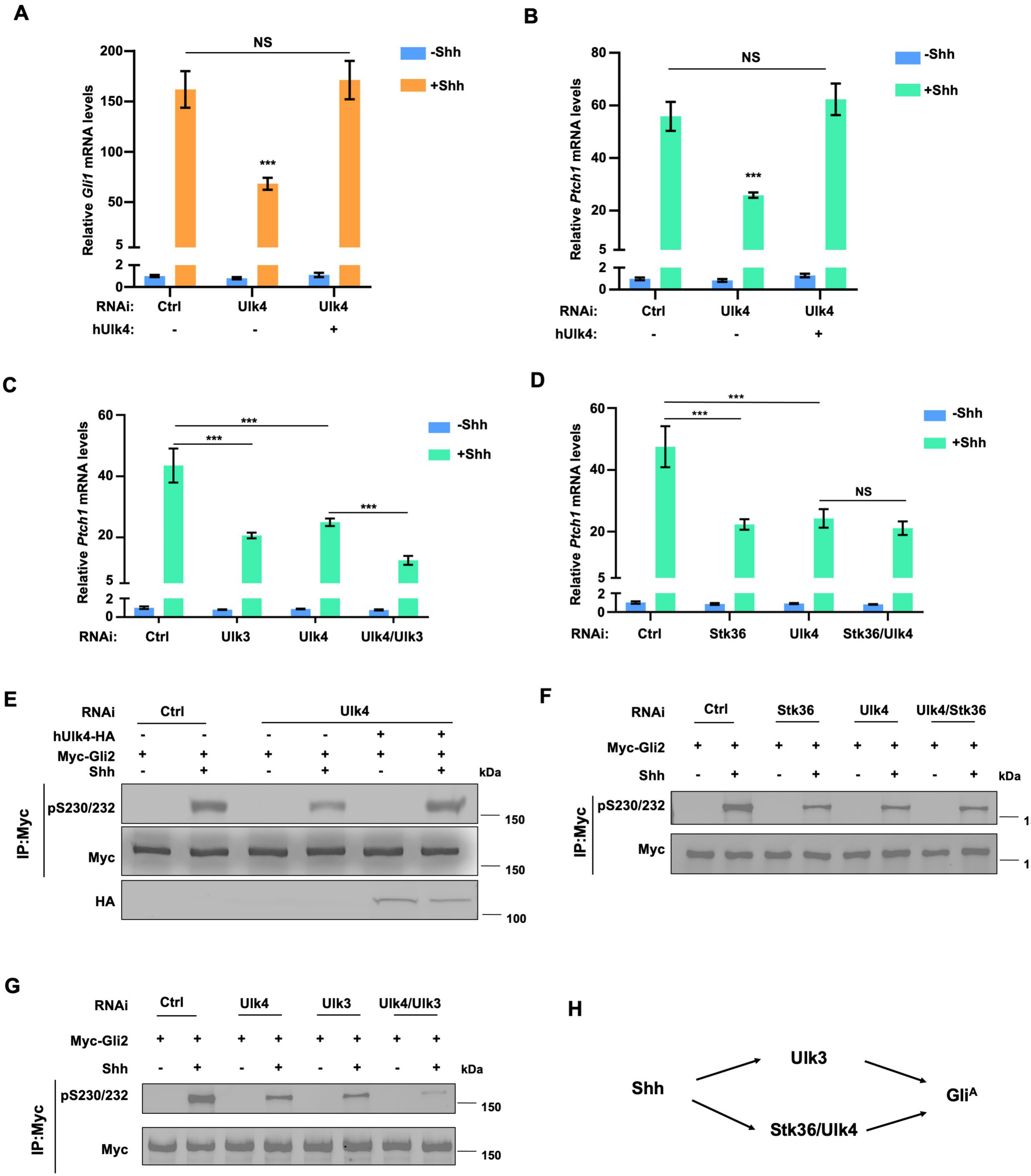
A
NS
***
-Shh
+Shh
Relative Gli1 mRNA levels
200
150
100
50
5
2
0
RNAi: Ctrl Ulk4 Ulk4
hUlk4: - - +
B
NS
***
-Shh
+Shh
Relative Ptch1 mRNA levels
80
60
40
20
5
2
0
RNAi: Ctrl Ulk4 Ulk4
hUlk4: - - +
C
***
***
***
-Shh
+Shh
Relative Ptch1 mRNA levels
60
40
20
5
2
0
RNAi: Ctrl Ulk3 Ulk4 Ulk4/Ulk3
D
***
***
NS
-Shh
+Shh
Relative Ptch1 mRNA levels
60
40
20
5
2
0
RNAi: Ctrl Stk36 Ulk4 Stk36/Ulk4
E
RNAi Ctrl Ulk4
hUlk4-HA - - - - + +
Myc-Gli2 + + + + + +
Shh - + - + - +
kDa
IP:Myc
pS230/232
Myc
HA
150
150
100
F
RNAi Ctrl Stk36 Ulk4 Ulk4/Stk36
Myc-Gli2 + + + + + + + +
Shh - + - + - + - +
kDa
IP:Myc
pS230/232
Myc
150
150
G
RNAi Ctrl Ulk4 Ulk3 Ulk4/Ulk3
Myc-Gli2 + + + + + + + +
Shh - + - + - + - +
kDa
IP:Myc
pS230/232
Myc
150
150
H
Shh
Ulk3
Stk36/Ulk4
GliA

Zhou_Fig2

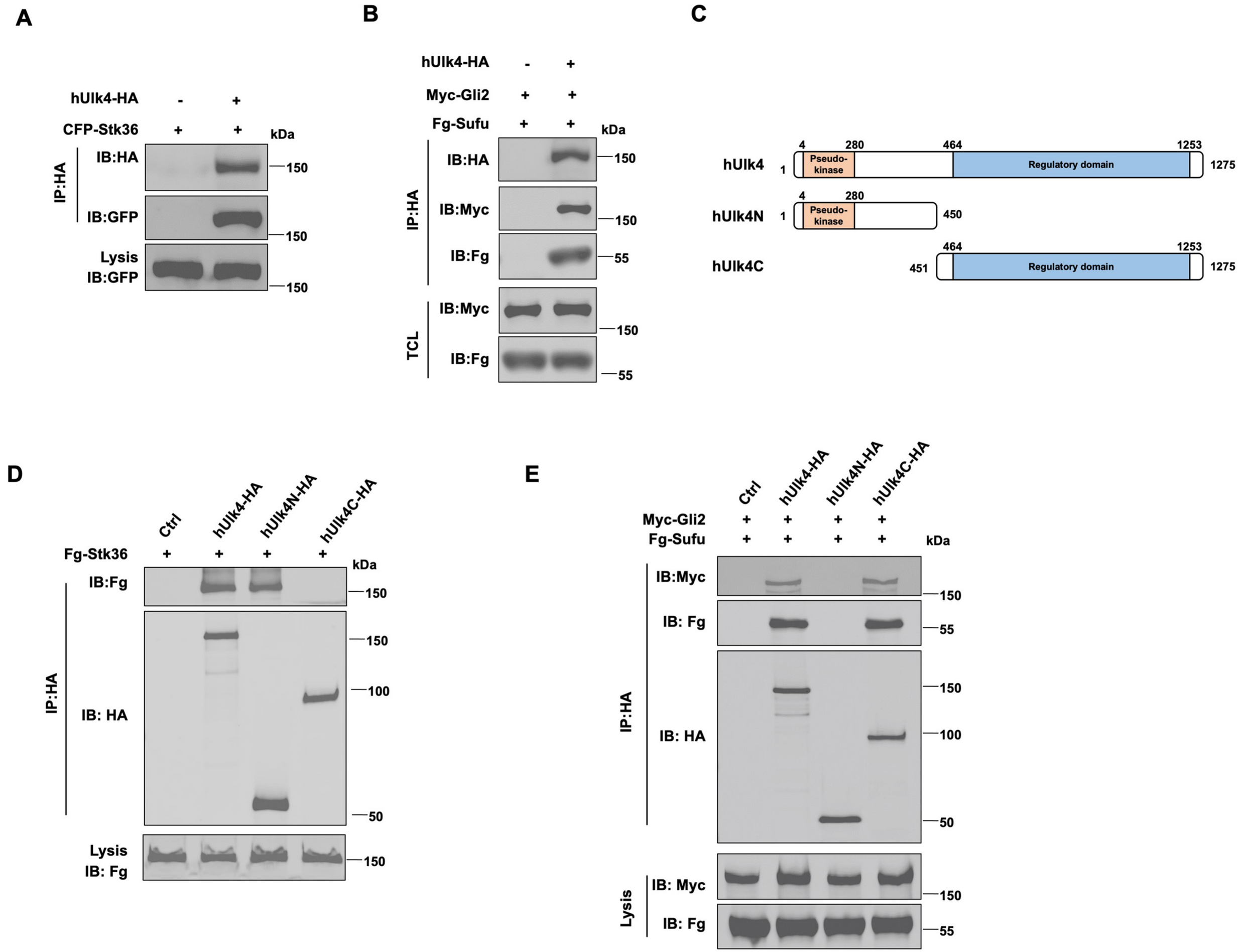
A
hUlk4-HA - +
CFP-Stk36 + +
kDa
IP:HA
IB:HA
150
IB:GFP
150
Lysis
IB:GFP
150
B
hUlk4-HA - +
Myc-Gli2 + +
Fg-Sufu + +
kDa
IP:HA
IB:HA
150
IB:Myc
150
IB:Fg
55
TCL
IB:Myc
150
IB:Fg
55
C
hUlk4
1
4
280
464
1253
1275
Pseudo-kinase
Regulatory domain
hUlk4N
1
4
280
450
Pseudo-kinase
hUlk4C
451
464
1253
1275
Regulatory domain
D
Ctrl
hUlk4-HA
hUlk4N-HA
hUlk4C-HA
Fg-Stk36 + + + +
kDa
IB:Fg
150
IP:HA
IB: HA
150
100
50
Lysis
IB: Fg
150
E
Ctrl
hUlk4-HA
hUlk4N-HA
hUlk4C-HA
Myc-Gli2 + + + +
Fg-Sufu + + + +
kDa
IP:HA
IB:Myc
150
IB: Fg
55
IB: HA
150
100
50
Lysis
IB: Myc
150
IB: Fg
55

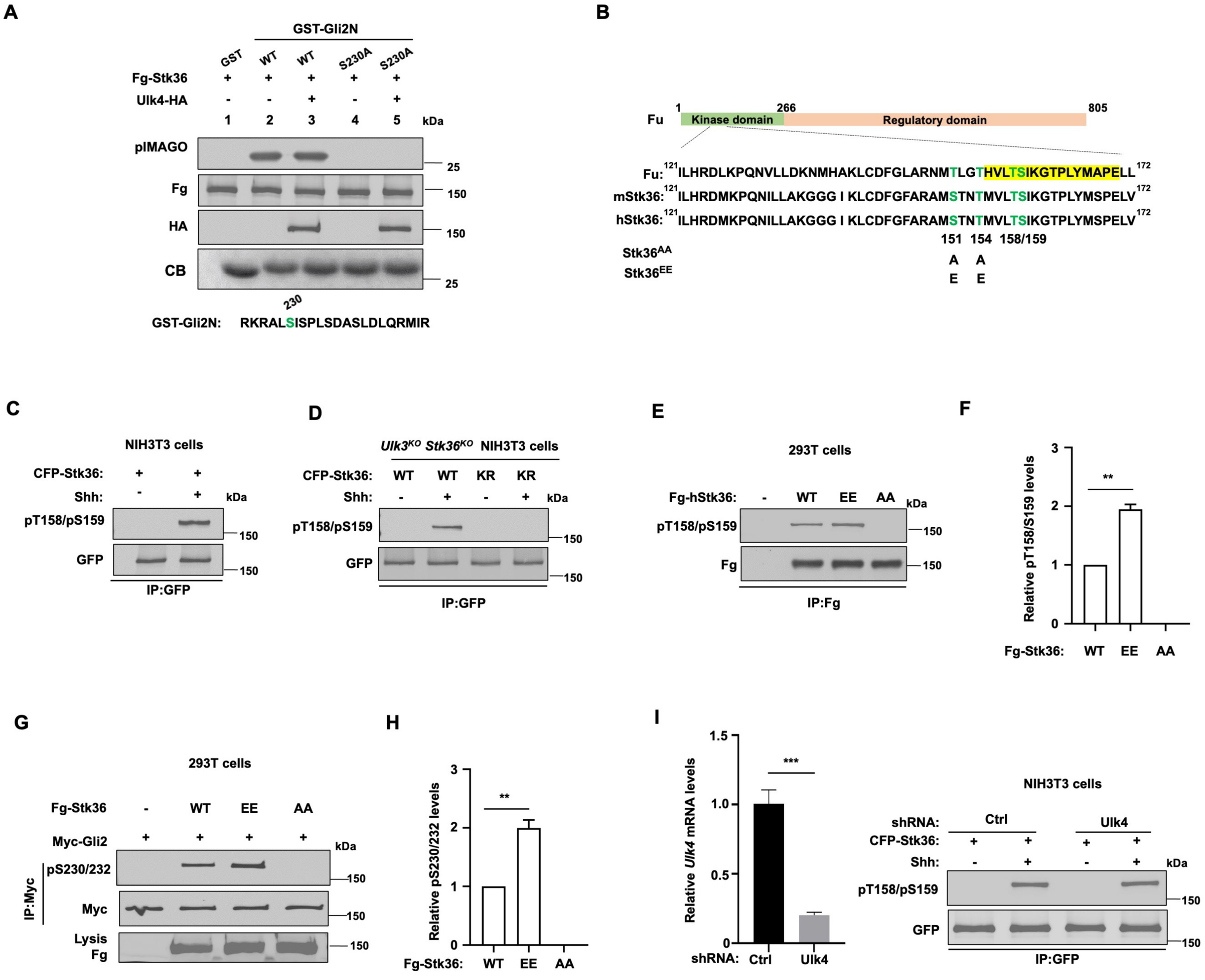
A
GST-Gli2N
GST
WT
WT
S230A
S230A
Fg-Stk36
Ulk4-HA
1 2 3 4 5 kDa
pIMAGO
Fg
HA
CB
25
150
150
25
230
GST-Gli2N: RKRALSISPLSDASLDLQRMIR
B
Fu
1
266
805
Kinase domain
Regulatory domain
Fu: 121 ILHRDLKPQNVLLDKNMHAKLCDFGLARNMTLGTHVLTSIKGTPLYMAPELL 172
mStk36: 121 ILHRDMKPQNILLAKGGG I KLCDFGFARAMSTNTMVLTSIKGTPLYMSPELV 172
hStk36: 121 ILHRDMKPQNILLAKGGG I KLCDFGFARAMSTNTMVLTSIKGTPLYMSPELV 172
151 154 158/159
Stk36AA
Stk36EE
A A
E E
C
NIH3T3 cells
CFP-Stk36: + +
Shh: - + kDa
pT158/pS159
GFP
150
150
IP:GFP
D
Ulk3KO Stk36KO NIH3T3 cells
CFP-Stk36: WT WT KR KR
Shh: - + - + kDa
pT158/pS159
GFP
150
150
IP:GFP
E
293T cells
Fg-hStk36: - WT EE AA kDa
pT158/pS159
Fg
150
150
IP:Fg
F
Relative pT158/S159 levels
3
2
1
0
**
Fg-Stk36: WT EE AA
G
293T cells
Fg-Stk36 - WT EE AA
Myc-Gli2 + + + + kDa
IP:Myc
pS230/232
Myc
Lysis Fg
150
150
150
H
Relative pS230/232 levels
3
2
1
0
**
Fg-Stk36: WT EE AA
I
Relative Ulk4 mRNA levels
1.5
1.0
0.5
0
***
shRNA: Ctrl Ulk4
NIH3T3 cells
shRNA: Ctrl Ulk4
CFP-Stk36: + + + +
Shh: - + - + kDa
pT158/pS159
GFP
150
150
IP:GFP

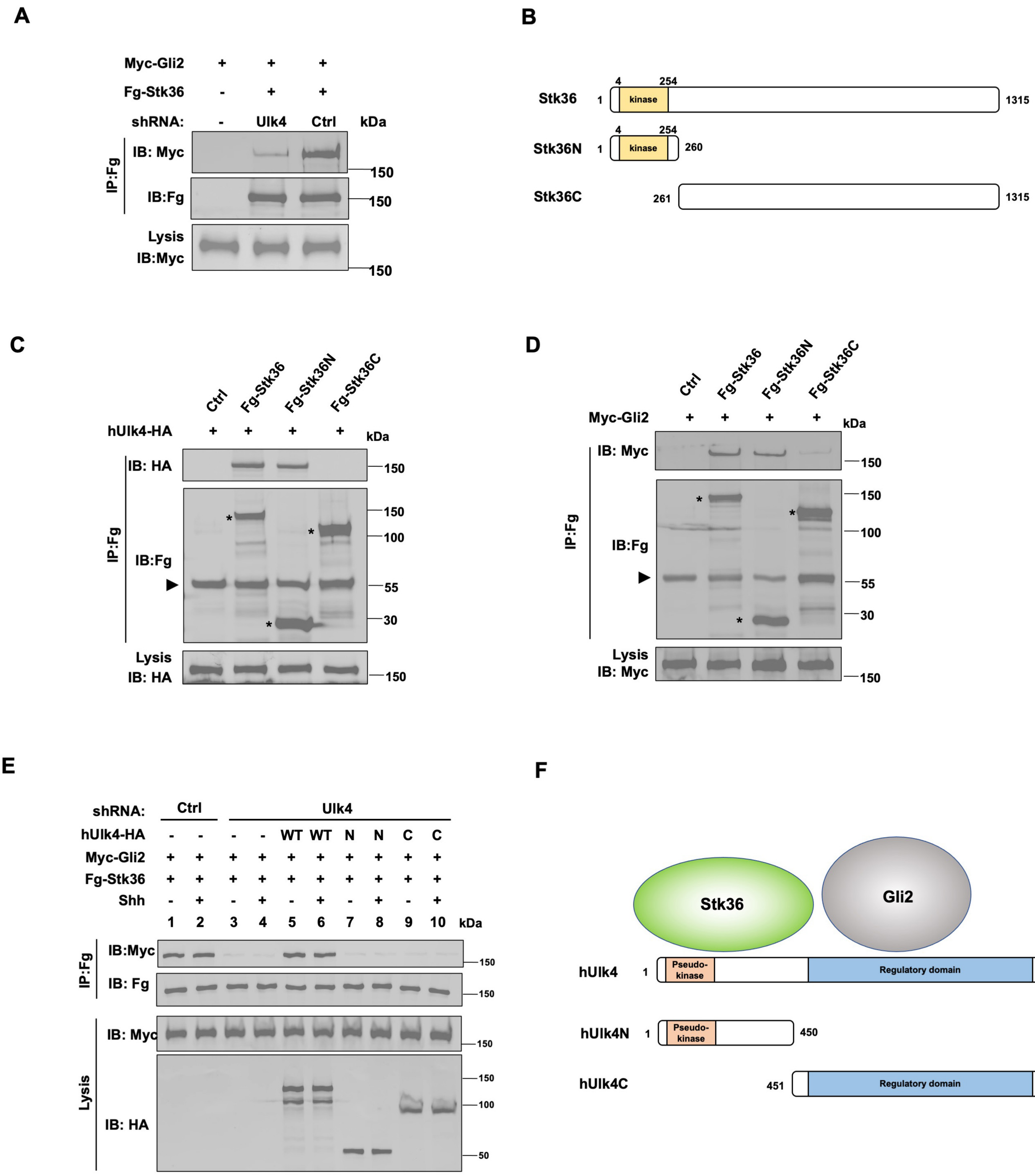
A
Myc-Gli2 + + +
Fg-Stk36 - + +
shRNA: - Ulk4 Ctrl kDa
IP:Fg
IB: Myc
IB:Fg
Lysis
IB:Myc
150
150
150
B
Stk36
Stk36N
Stk36C
kinase
4
254
1
1315
260
261
C
Ctrl
Fg-Stk36
Fg-Stk36N
Fg-Stk36C
hUlk4-HA + + + +
kDa
IB: HA
IB:Fg
Lysis
IB: HA
150
100
55
30
D
Myc-Gli2 + + + +
IB: Myc
IB:Fg
Lysis
IB: Myc
E
shRNA: Ctrl Ulk4
hUlk4-HA - - - - WT WT N N C C
Myc-Gli2 + + + + + + + + + +
Fg-Stk36 + + + + + + + + + +
Shh - + - + - + - + - +
1 2 3 4 5 6 7 8 9 10 kDa
IP:Fg
IB:Myc
IB: Fg
Lysis
IB: Myc
IB: HA
150
100
50
F
Stk36
Gli2
hUlk4
hUlk4N
hUlk4C
Pseudo-kinase
Regulatory domain
1
1275
450
451

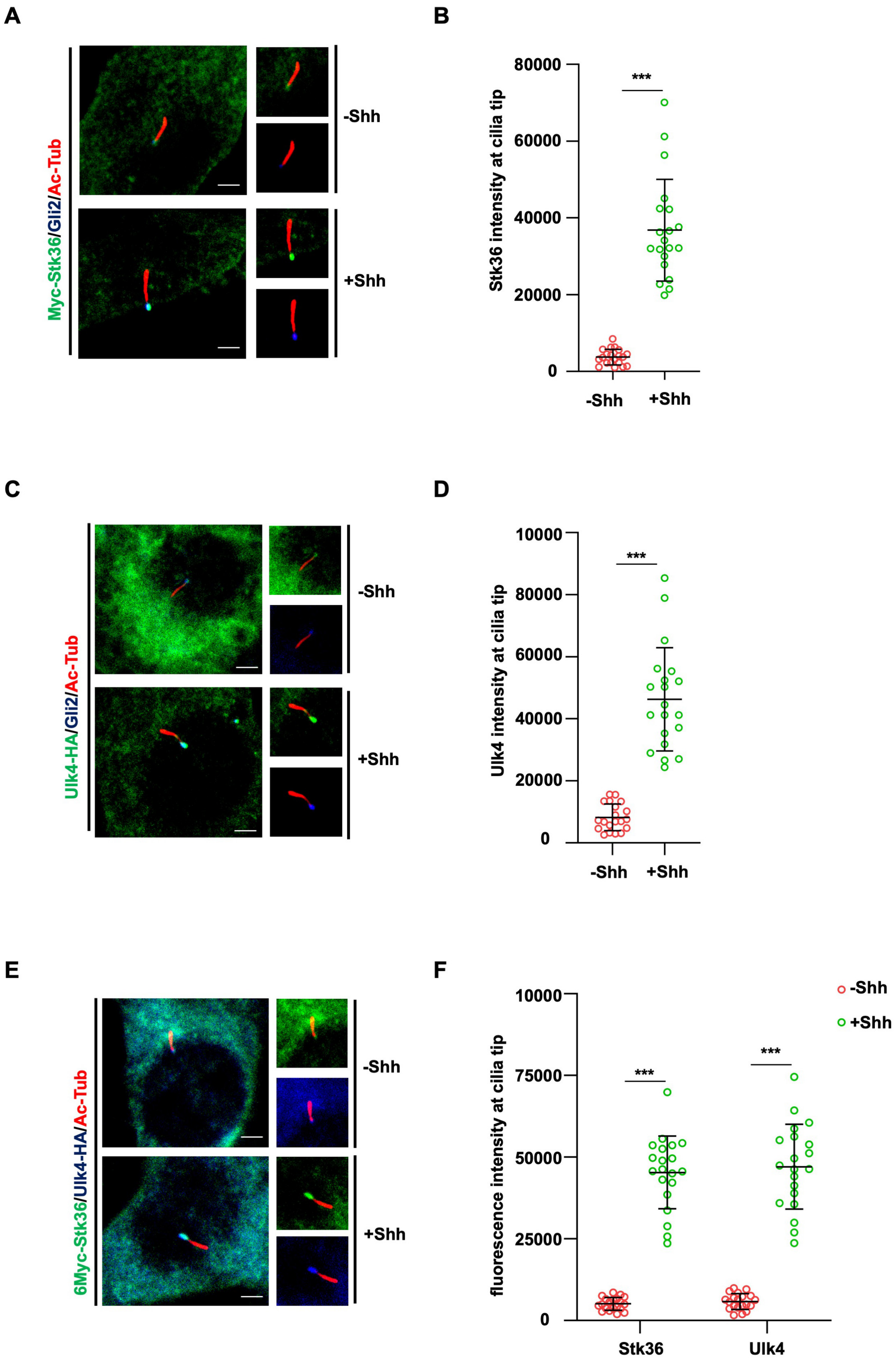
A
Myc-Stk36/Gli2/Ac-Tub
-Shh
+Shh
B
Stk36 intensity at cilia tip
80000
60000
40000
20000
0
***
-Shh
+Shh
C
Ulk4-HA/Gli2/Ac-Tub
-Shh
+Shh
D
Ulk4 intensity at cilia tip
10000
80000
60000
40000
20000
0
***
-Shh
+Shh
E
6Myc-Stk36/Ulk4-HA/Ac-Tub
-Shh
+Shh
F
fluorescence intensity at cilia tip
10000
75000
50000
25000
0
***
***
-Shh
+Shh
Stk36
Ulk4

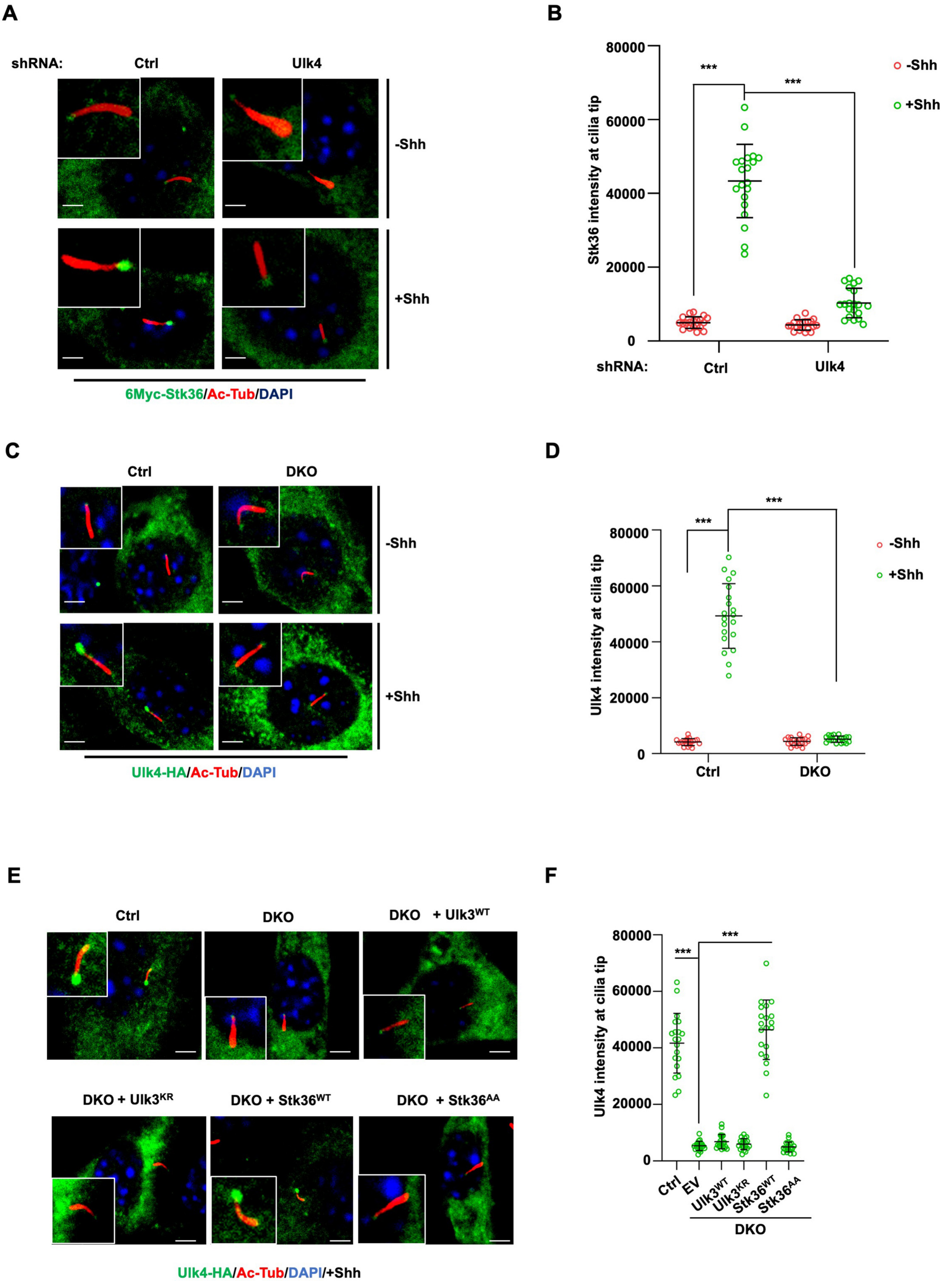
A
shRNA:
Ctrl
Ulk4
-Shh
+Shh
6Myc-Stk36/Ac-Tub/DAPI
B
Stk36 intensity at cilia tip
80000
60000
40000
20000
0
***
***
-Shh
+Shh
shRNA:
Ctrl
Ulk4
C
Ctrl
DKO
-Shh
+Shh
Ulk4-HA/Ac-Tub/DAPI
D
Ulk4 intensity at cilia tip
80000
60000
40000
20000
0
***
***
-Shh
+Shh
Ctrl
DKO
E
Ctrl
DKO
DKO + Ulk3WT
DKO + Ulk3KR
DKO + Stk36WT
DKO + Stk36AA
Ulk4-HA/Ac-Tub/DAPI/+Shh
F
Ulk4 intensity at cilia tip
80000
60000
40000
20000
0
***
***
Ctrl
EV
Ulk3WT
Ulk3KR
Stk36WT
Stk36AA
DKO

A

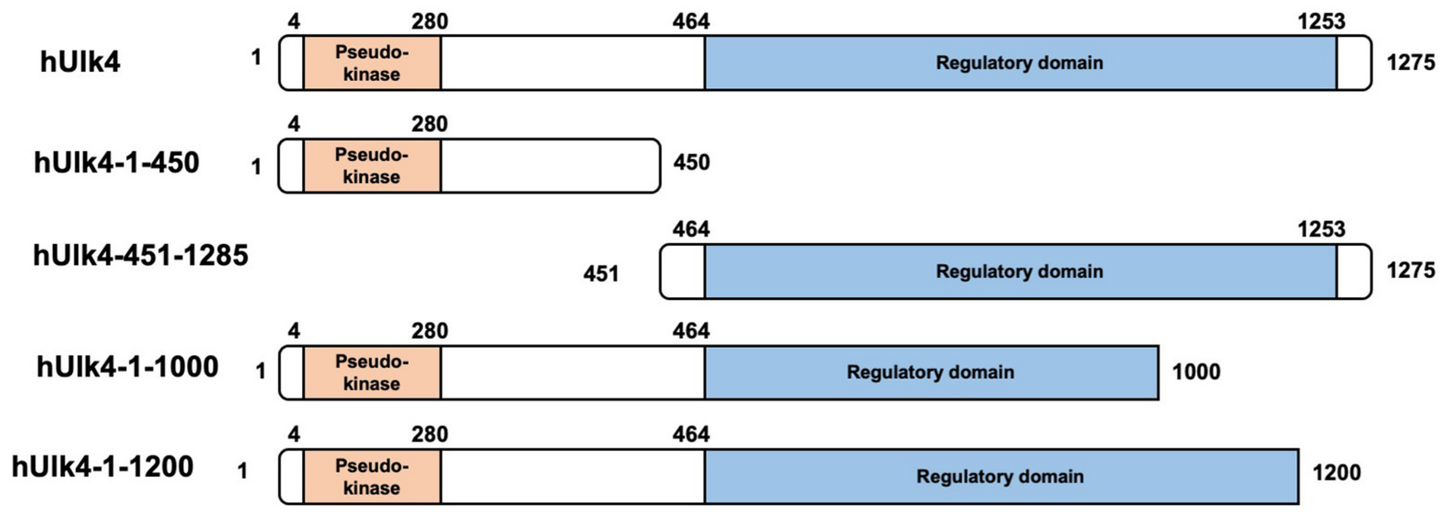
hUlk4
1
4
280
464
1253
1275
Pseudo-kinase
Regulatory domain
hUlk4-1-450
450
hUlk4-451-1285
451
hUlk4-1-1000
1000
hUlk4-1-1200
1200

B

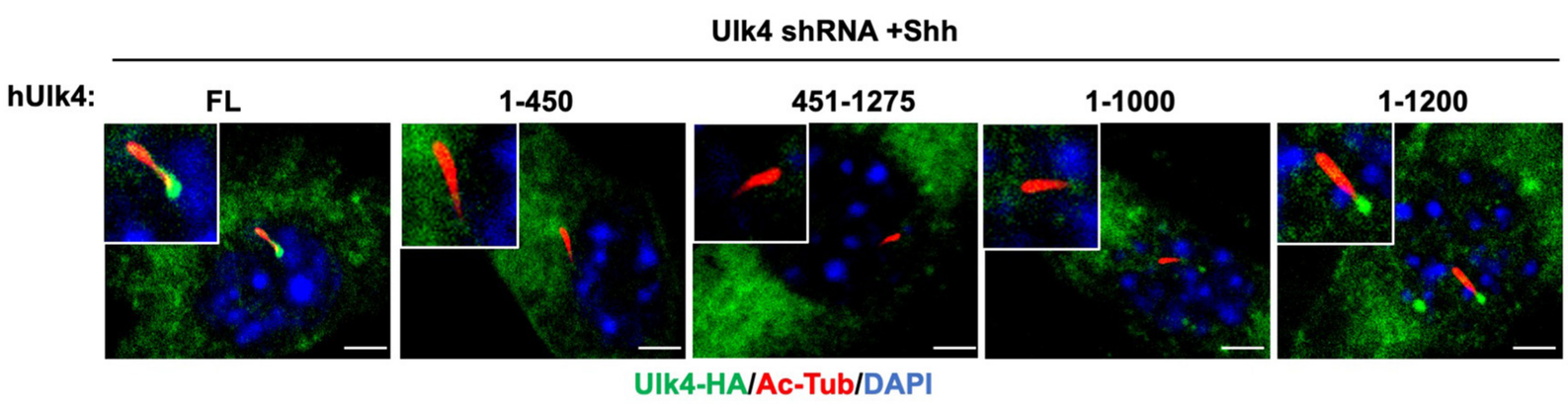
Ulk4 shRNA +Shh
hUlk4:
FL
1-450
451-1275
1-1000
1-1200
Ulk4-HA/Ac-Tub/DAPI

C

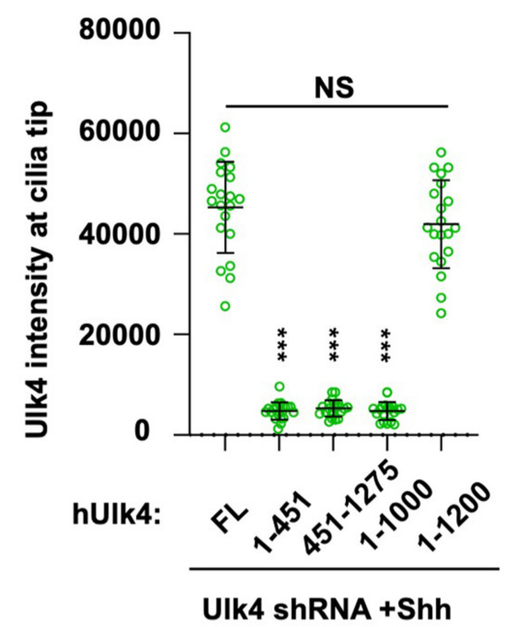
Ulk4 intensity at cilia tip
80000
60000
40000
20000
0
NS
***
***
***
hUlk4:
FL
1-451
451-1275
1-1000
1-1200
Ulk4 shRNA +Shh

D

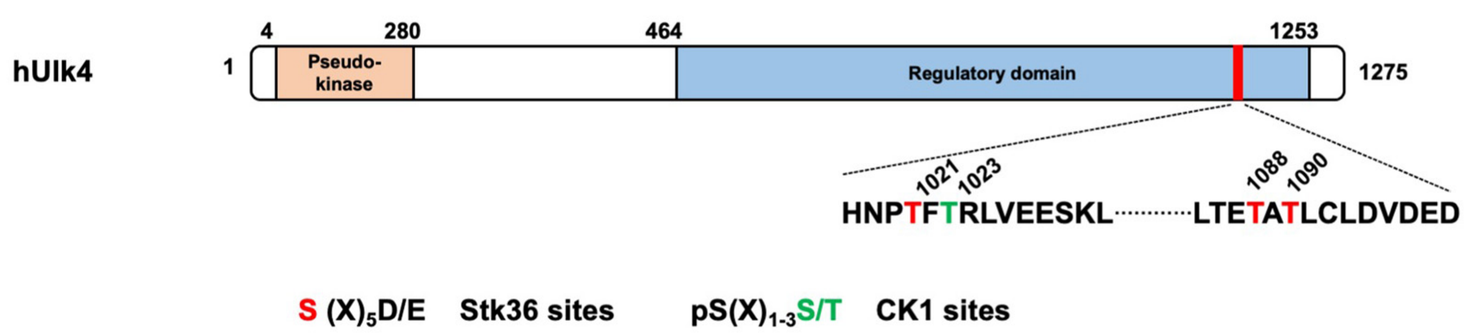
hUlk4
1
4
280
464
1253
1275
Pseudo-kinase
Regulatory domain
1021
1023
1088
1090
HNPTFTRLVEESKL
LTETATLCLDVDED
S (X)5D/E Stk36 sites
pS(X)1-3S/T CK1 sites

E

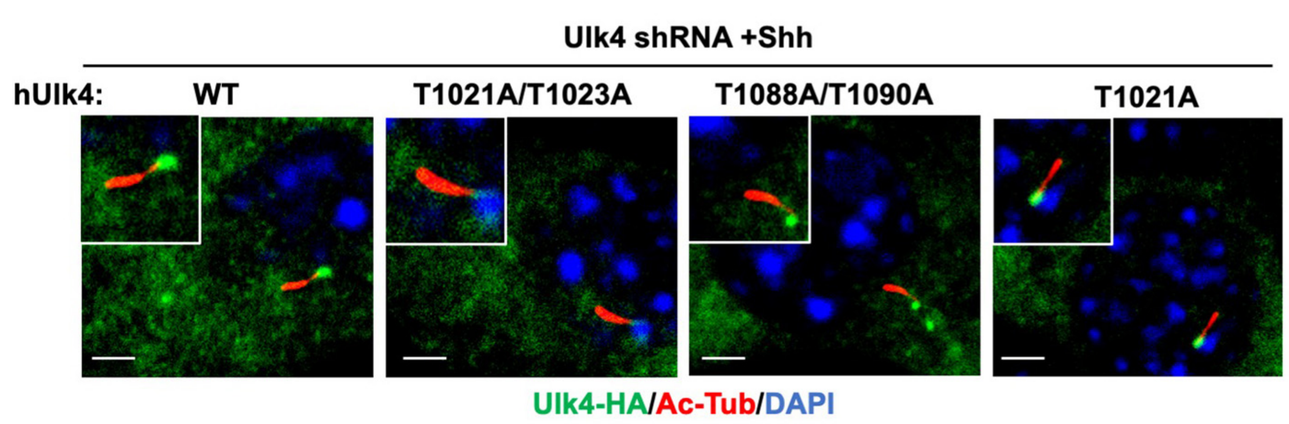
Ulk4 shRNA +Shh
hUlk4:
WT
T1021A/T1023A
T1088A/T1090A
T1021A
Ulk4-HA/Ac-Tub/DAPI

F

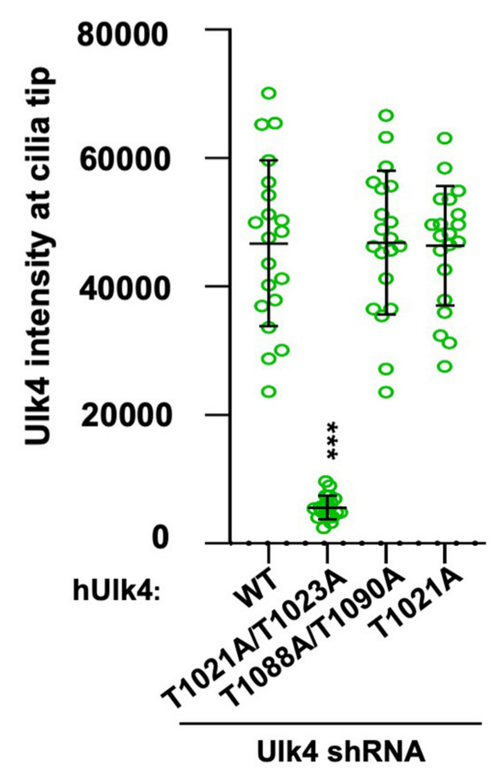
Ulk4 intensity at cilia tip
80000
60000
40000
20000
0
***
hUlk4:
WT
T1021A/T1023A
T1088A/T1090A
T1021A
Ulk4 shRNA

G

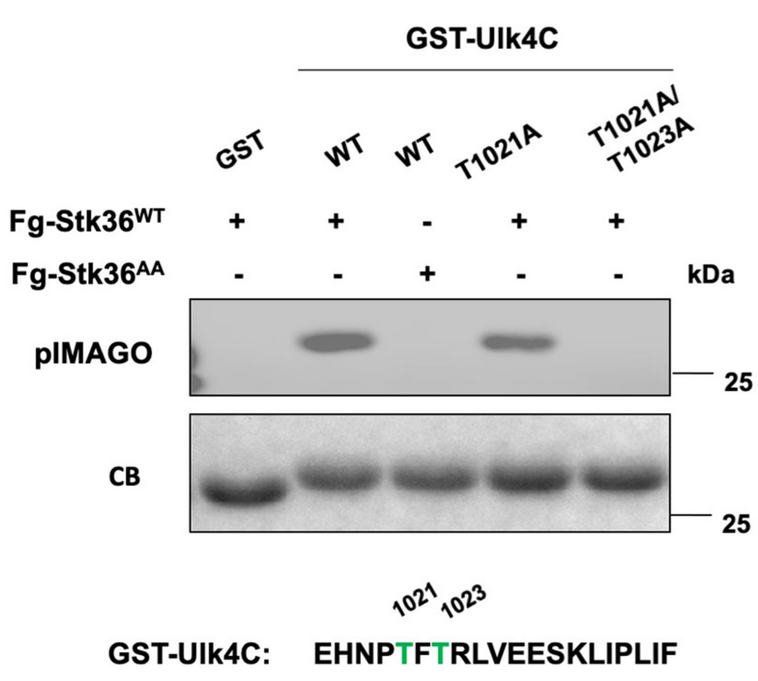
GST-Ulk4C
GST
WT
WT
T1021A
T1021A/T1023A
Fg-Stk36WT + + - + +
Fg-Stk36AA - - + - -
kDa
pIMAGO
25
CB
25
1021
1023
GST-Ulk4C: EHNPTFTRLVEESKLIPLIF

H

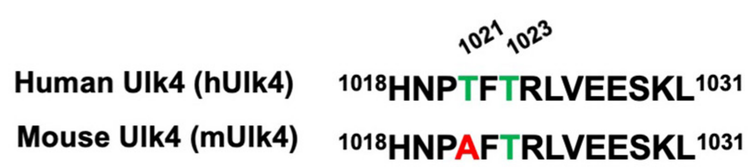
1021
1023
Human Ulk4 (hUlk4) 1018HNPTFTRLVEESKL1031
Mouse Ulk4 (mUlk4) 1018HNPAFTRLVEESKL1031

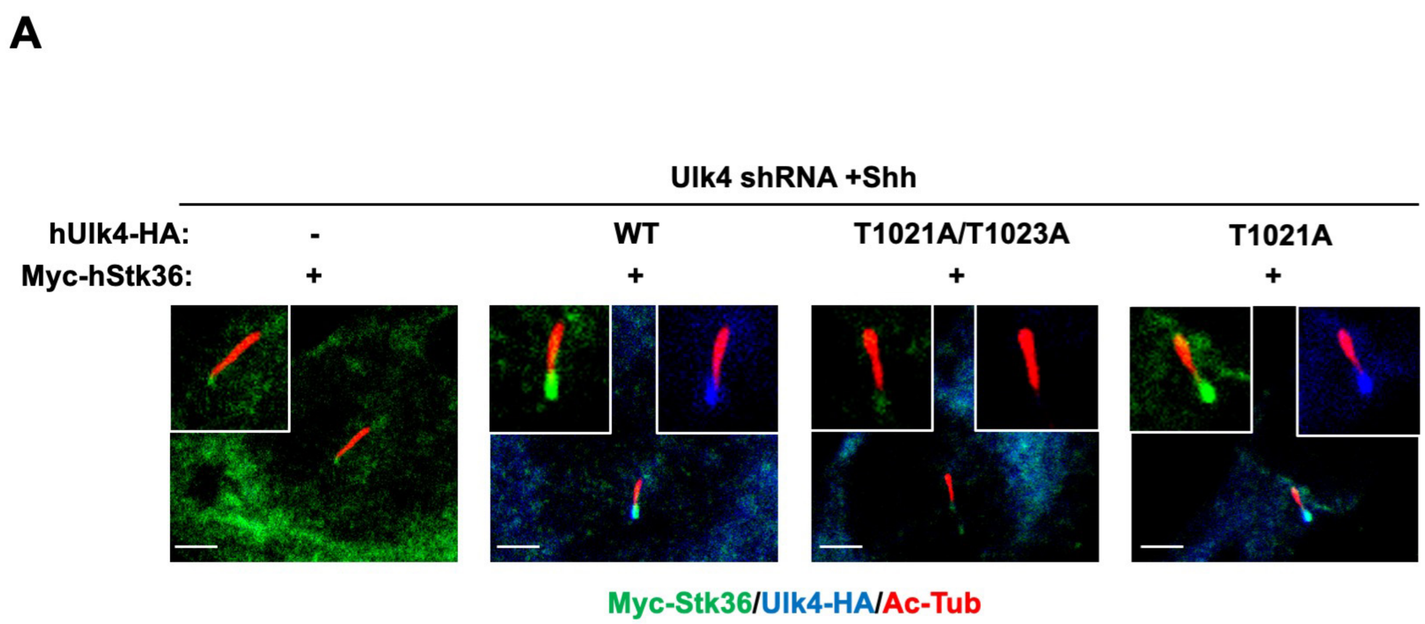
A
Ulk4 shRNA +Shh
hUlk4-HA: - WT T1021A/T1023A T1021A
Myc-hStk36: + + + +
Myc-Stk36/Ulk4-HA/Ac-Tub

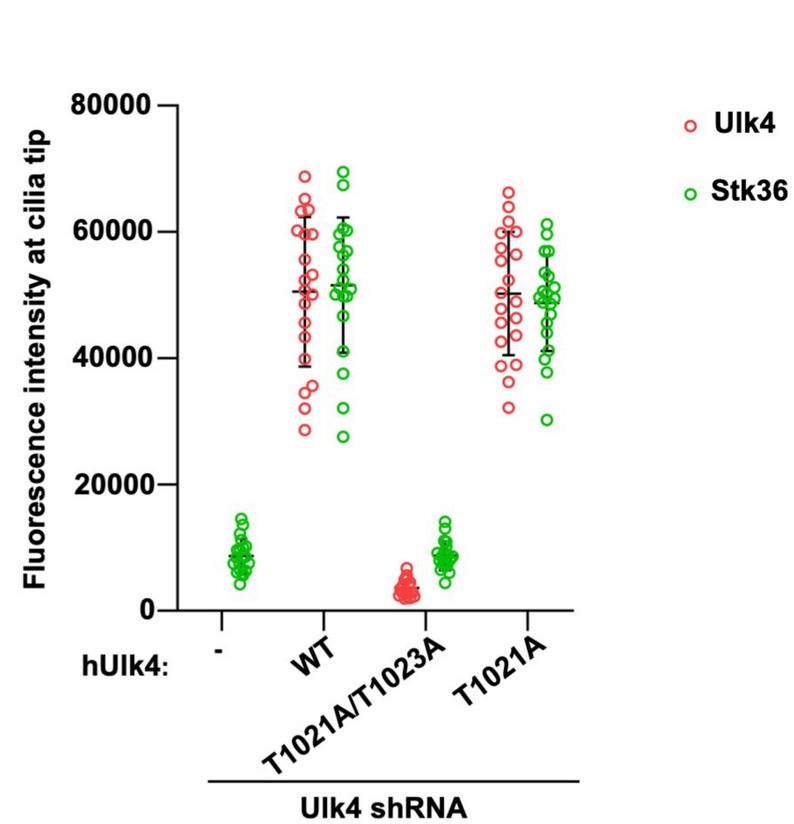
B
Fluorescence intensity at cilia tip
80000
60000
40000
20000
0
Ulk4
Stk36
hUlk4: - WT T1021A/T1023A T1021A
Ulk4 shRNA

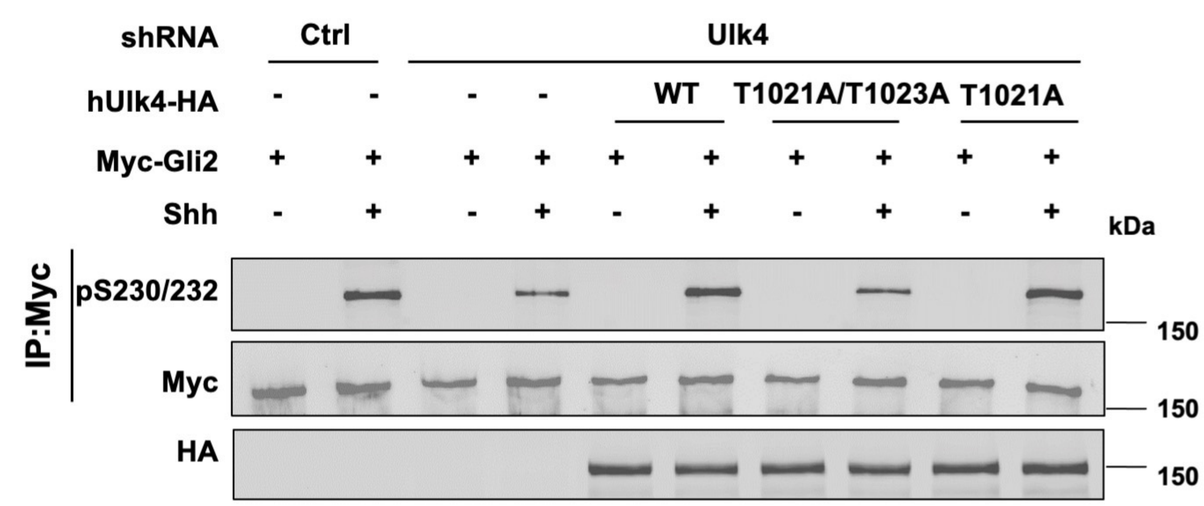
C
shRNA Ctrl Ulk4
hUlk4-HA - - - - WT T1021A/T1023A T1021A
Myc-Gli2 + + + + + + + + + +
Shh - + - + - + - + - +
kDa
IP:Myc
pS230/232
Myc
HA
150
150
150

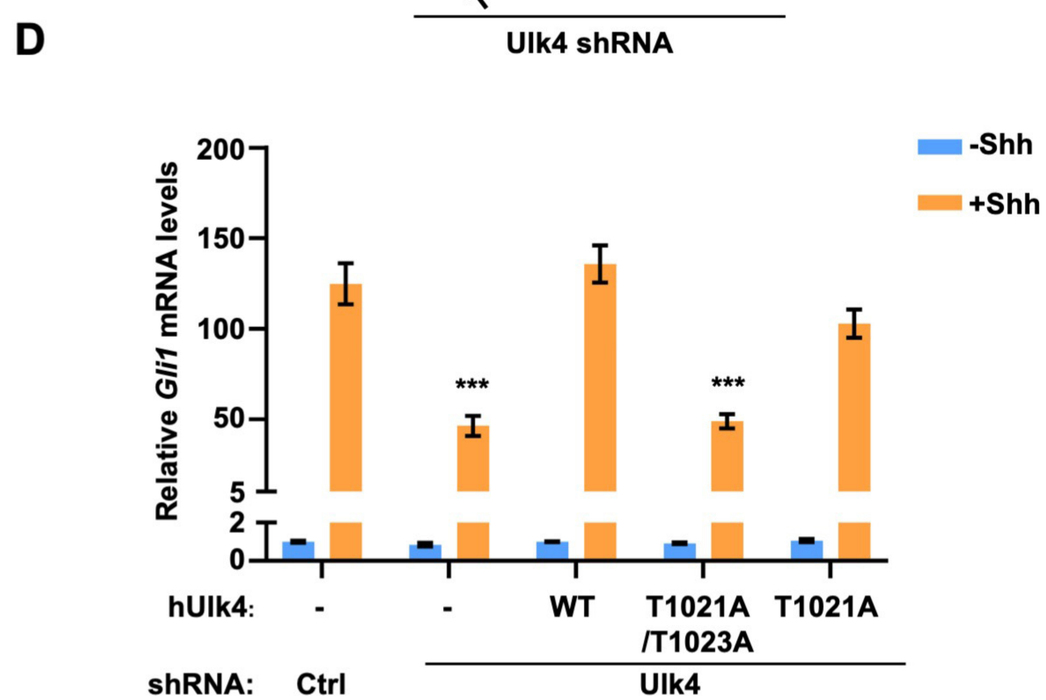
D
Relative Gli1 mRNA levels
200
150
100
50
5
2
0
-Shh
+Shh
***
***
hUlk4: - - WT T1021A /T1023A T1021A
shRNA: Ctrl Ulk4

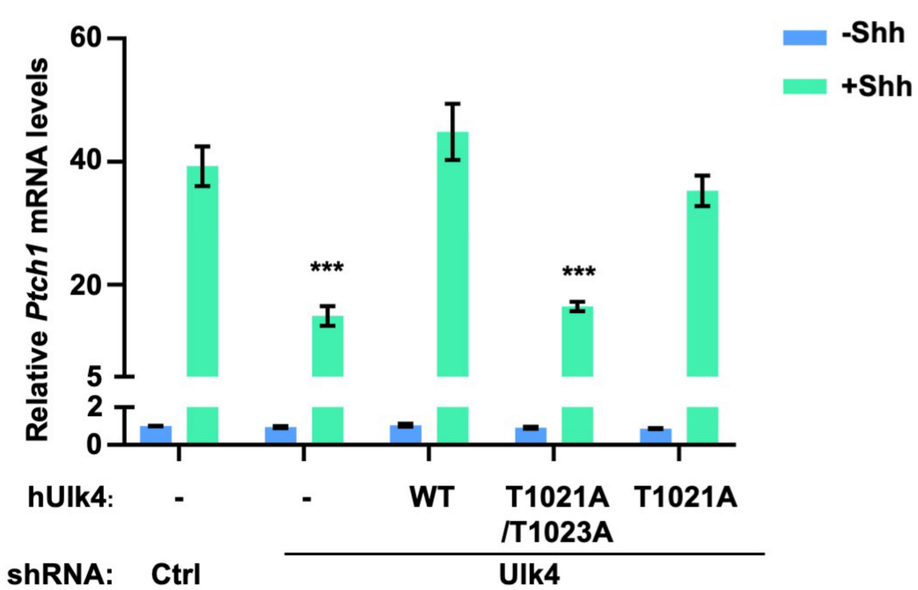
E
Relative Ptch1 mRNA levels
60
40
20
5
2
0
-Shh
+Shh
***
***
hUlk4: - - WT T1021A /T1023A T1021A
shRNA: Ctrl Ulk4

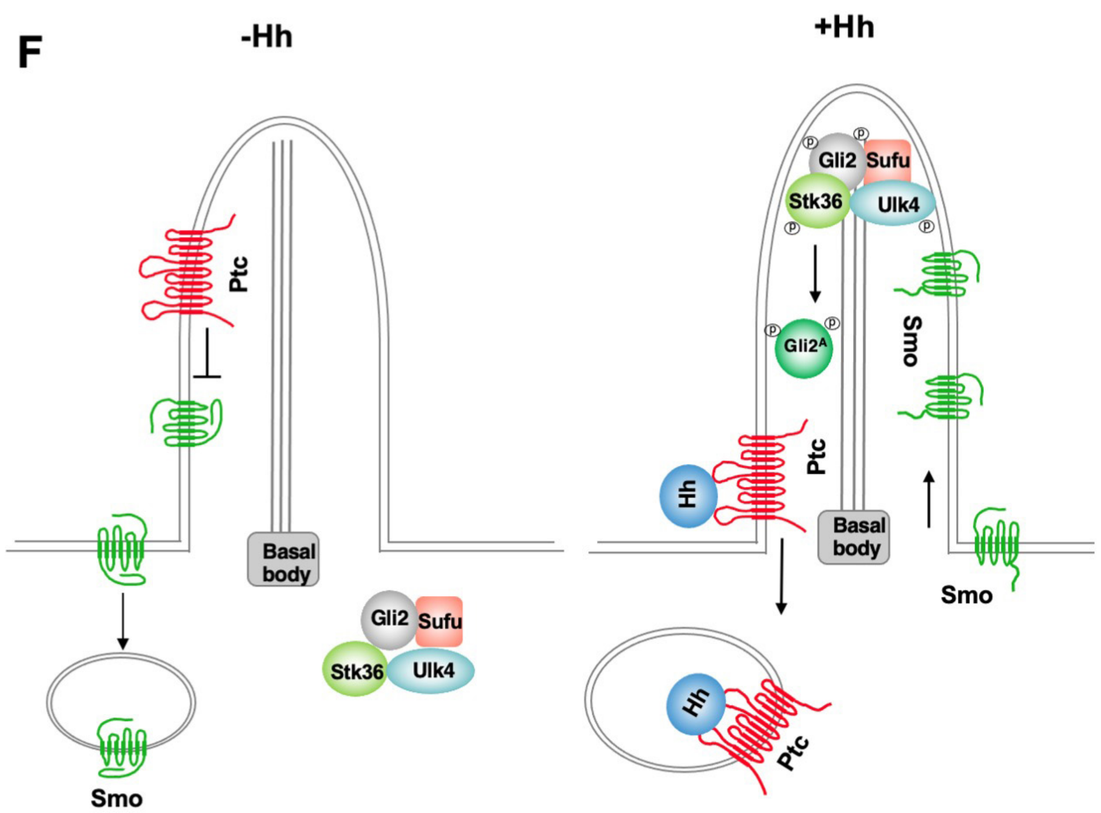
F
-Hh
+Hh
Ptc
Basal body
Gli2
Sufu
Stk36
Ulk4
Smo
Gli2A
Hh

Fig1_figure supplement 1

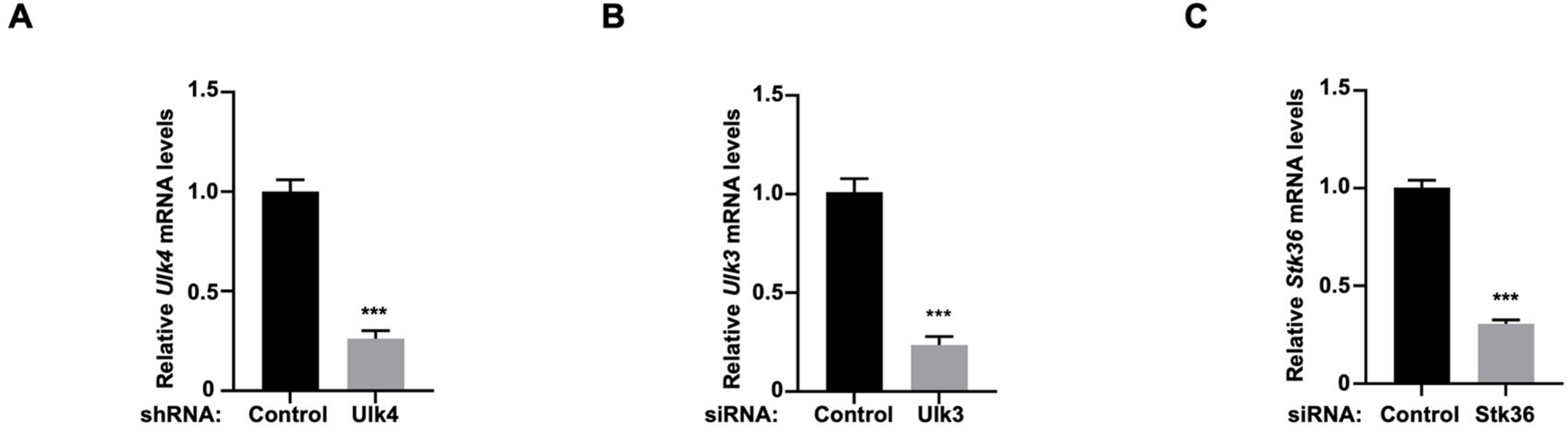
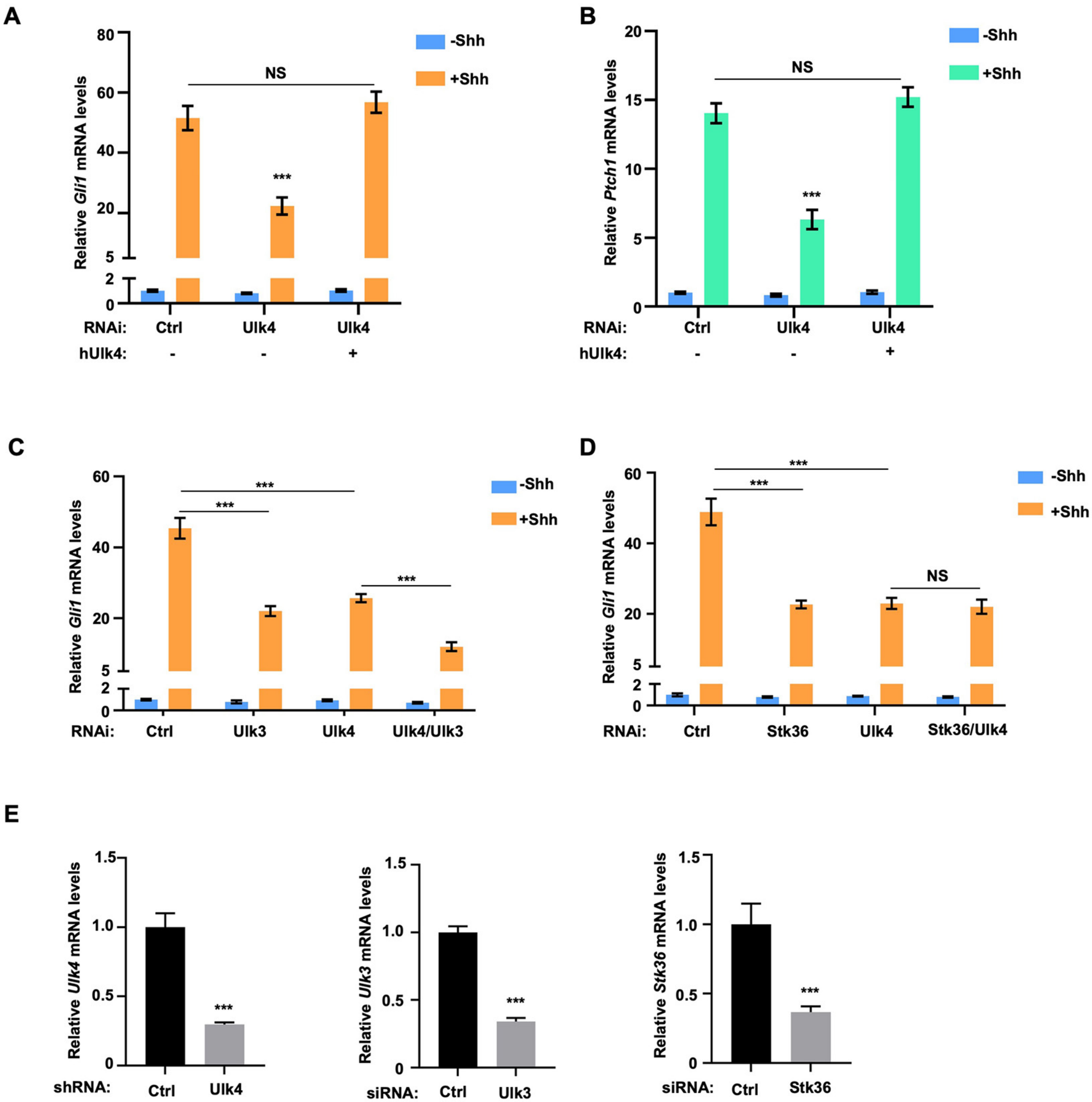
Fig1_figure supplement 2